Eur. Phys. J. A **24**, 293–312 (2005)
DOI 10.1140/epja/i2004-10142-5

THE EUROPEAN PHYSICAL JOURNAL A

Neutron stars in a Skyrme model with hyperons

L. Mornas[a]

Departamento de Física, Universidad de Oviedo, Avda Calvo Sotelo 18, 33007 Oviedo, Spain

Received: 9 August 2004 / Revised version: 15 February 2005 /
Published online: 19 April 2005 –
Communicated by V. Vento

Abstract. Available Skyrme parametrizations with hyperons are examined from the point of view of their suitability for applications to neutron stars. It is shown that the hyperons can attenuate or even remove the problem of ferromagnetic instability common to (nearly) all Skyrme parametrizations of the nucleon-nucleon interaction. At high density the results are very sensitive to the choice of the $\Lambda\Lambda$ interaction. The selected parameter sets are then used to obtain the resulting properties of both cold neutron stars and hot protoneutron stars. The general features known from other models are recovered.

PACS. 97.60.Jd Neutron stars – 21.65.+f Nuclear matter – 21.30.-x Nuclear forces

1 Introduction

Skyrme parametrizations provide a simple tool for calculating the equation of state. Skyrme or Skyrme-inspired models are often used in applications to neutron stars with adapted versions which pay special attention to the asymmetry properties. The Skyrme Lyon series [1] is the most modern example of this approach and was designed to reproduce saturation properties, the main properties of nuclei as well as the results of simulations of pure neutron matter.

In neutron stars in chemical equilibrium, hyperons appear at a threshold density about twice the nuclear saturation density. A sizable hyperon fraction can be expected to be present in the core of the most massive neutron stars; the central density of the Skyrme Lyon series, for example, is of the order of seven times saturation density in the star with maximum mass and three to four times saturation density in a 1.4 $M_\odot$ star.

Original Skyrme parametrizations did not take hyperons into account. Balberg and Gal [2] have remedied the fact with their parametrization of the energy density. It could be argued, however, that the description of the nucleon sector provided by this parametrization is rather poor.

Rather than designing a new force in the hyperonic sector with the purpose of describing neutron stars, another possibility would be to restrict oneself to the numerous available data sets which were fitted to nuclear properties. This is the approach taken by Rikovska Stone *et al.* [3], who recently tested 87 parameter sets for the NN force in neutron star calculations.

[a] e-mail: lysiane@pinon.ccu.uniovi.es

In the hyperonic sector there exist a few parametrizations of the Lambda-Nucleon and Lambda-Lambda interaction fitted to the properties of hypernuclei, including several well-tested sets by Lanskoy *el al.* [4,5] and an earlier set by Fernandez *et al.* [6]. The present work can be considered as an extension of the study of Rikovska Stone *et al.* including the Λ-hyperon.

A general feature of Skyrme models in the np sector is that they show a ferromagnetic transition at rather low density [7,8]. If present, such a transition, apart from modifying the equation of state and chemical equilibrium, could give rise to induced magnetic fields in rotating neutron stars. It also plays a crucial role in calculations of the neutrino mean free path in supernova and protoneutron stars. Calculations of this parameter in non-relativistic (Skyrme or Gogny) models of nuclear matter [9–11] thus obtained that the cross-section diverges and the mean free path drops to zero at the transition.

It remains an open issue whether this transition is genuine or an artefact of the Skyrme model. While a free Fermi gas eventually becomes ferromagnetic, the nuclear correlations are known to play a crucial role. Most non-relativistic calculations which take correlations into account, *e.g.* by solving the Brueckner-Hartree-Fock equations with modern bare NN potentials [12,13], concluded that spin ordered matter was not favored energetically. Relativistic mean-field models predict no ferromagnetic transition; on the other hand, relativistic calculations in the Hartree-Fock approximation by Bernardos *et al.* [14] find a transition, albeit as a rather large density (4 $n_{\rm sat}$). A recent work by Maruyama and Tatsumi [15], although not putting forward a quantitative prediction, reaches a

similar conclusion as to the importance of the Fock contribution.

In this work we will take the viewpoint that the ferromagnetic transition, especially when appearing at such low densities as 2-3 times saturation, is probably an artefact of the Skyrme model, and will select among the available Skyrme parametrizations those which as far as possible avoid or delay the transition to higher densities.

This work includes the effects of temperature and neutrino trapping and can also be applied in hot protoneutron stars.

A further motivation of the present study was to obtain a model which would allow to calculate the neutrino-baryon scattering rate in the hot protoneutron star formed shortly after the supernova collapse. It was therefore necessary to be able to calculate the Landau parameters in the spin $S = 1$ channel. Besides determining the position of an eventual ferromagnetic transition, the Landau parameters in the spin $S = 1$ channel play a central role when calculating the axial response function in the random phase approximation, which is the dominant contribution to the neutrino-baryon scattering rate. This application has been presented in a separate paper [16].

After a presentation of the available Skyrme parametrizations in sect. 2, the following sections proceed to select a few among them according to their suitability for neutron star applications. Section 3 first examines the threshold density for hyperon formation under the conditions of β equilibrium. Section 4 presents a discussion of the issue of ferromagnetism. The selected parameter sets are used in sect. 5 to obtain the properties of the corresponding neutron stars. In sect. 6 some approximations of the model (neglect of μ, Σ^-) are re-examined. The effect of non-vanishing temperature and of a trapped neutrino fraction are studied in sect. 7. The main results are collected and discussed in the conclusion.

The formalism is kept to a minimum in the main text, while all relevant formulae are gathered in the appendix.

2 Skyrme parametrizations of the hyperonic sector

The usual Skyrme model of nuclear matter introduces the nucleon-nucleon potential

$$\begin{aligned} V_{NN}(r_1 - r_2) &= t_0\,(1 + x_0 P_\sigma)\delta(r_1 - r_2) \\ &+\frac{1}{2}t_1\,(1 + x_1 P_\sigma)\left[k'^2\ \delta(r_1 - r_2) + \delta(r_1 - r_2)\ k^2\right] \\ &+t_2\,(1 + x_2 P_\sigma)k'\,\delta(r_1 - r_2)\,k \\ &+\frac{1}{6}t_3\,(1 + x_3 P_\sigma)\,\rho_N^\alpha\left(\frac{r_1 + r_2}{2}\right)\delta(r_1 - r_2)\,. \end{aligned} \tag{1}$$

It can readily be generalized to include nucleon-Lambda and Lambda-Lambda interaction potentials (see, *e.g.*, [4,5])

$$\begin{aligned} V_{N\Lambda}(r_N - r_\Lambda) &= u_0\,(1 + y_0 P_\sigma)\delta(r_N - r_\Lambda) \\ &+\frac{1}{2}u_1\,\left[k'^2\ \delta(r_N - r_\Lambda) + \delta(r_N - r_\Lambda)\ k^2\right] \\ &+u_2\,k'\,\delta(r_N - r_\Lambda)\,k + \frac{3}{8}u_3\,(1 + y_3 P_\sigma) \\ &\times\rho_N^\beta\left(\frac{r_N + r_\Lambda}{2}\right)\delta(r_N - r_\Lambda) \end{aligned} \tag{2}$$

$$\begin{aligned} V_{\Lambda\Lambda}(r_1 - r_2) &= \lambda_0\delta(r_1 - r_2) \\ &+\frac{1}{2}\lambda_1\,\left[k'^2\ \delta(r_1 - r_2) + \delta(r_1 - r_2)\ k^2\right] \\ &+\lambda_2\,k'\,\delta(r_1 - r_2)\,k + \lambda_3\,\rho_\Lambda\rho_N^\gamma \end{aligned} \tag{3}$$

The potentials normally also include spin orbit contributions. They are not explicited here since they will not be used in the remainder of this paper.

The energy density is then obtained in the Hartree-Fock approximation from

$$\begin{aligned} \mathcal{E} &= \langle\psi\,|\,H\,|\,\psi\rangle \quad \text{with} \quad H = \sum_{A=N,\Lambda} T_A + \frac{1}{2}\sum_{A,B=N,\Lambda} V_{AB} \\ &= \mathcal{E}_{NN} + \mathcal{E}_{N\Lambda} + \mathcal{E}_{\Lambda\Lambda} \end{aligned} \tag{4}$$

In homogeneous matter the wave functions are formed from antisymmetrized plane wave states. The explicit expression of the energy density is given in the appendix.

In our search for some suitable sets of Skyrme parametrizations we have tested 44 NN Skyrme forces in combination with 13 parametrizations of the $N\Lambda$ and 4 options for the $\Lambda\Lambda$ forces. The NN forces were chosen among: SIII, SkM*, SI′, SIII′, SV, RATP, SGI, SGII, SLy230a, SLy2, SLy4, SLy5, SLy6, SLy7, SLy9, SLy10, SkO, SkO′, SkS3, SkI1, SkI2, SkI3, SkI4, SkI5, Rs, Gs, SkT4, SkT5, T6, SkP, Ska, MSka, SK272, SK255, Skz-0, Skz-1, Skz-2, Skz-3, Skz-4, SkSc4, SkSC6, SkSc15, MSk7, SKX. After demanding that these sets fulfill various constraints that will be discussed in detail in the next two sections, only four NN forces were sorted out: the SLy10 force from the Skyrme-Lyon series [1], the modern SkI3 and SkI5 forces by Reinhard and Flocard [17] and the older SV force by Beiner *et al.* [18].

For the nucleon-Λ interaction we have tried several parameter sets given by Lanskoy and Yamamoto [4,19] and by Fernandez *et al.* [6]: The $N\Lambda$ sets numbered from I to V in [4] are named LYI-LYV here, the sets numbered from 1 to 6 in [19] are named YBZ1-YBZ6, other choices are the SkSH1 and SkSH2 sets of [6] or to switch off the $N\Lambda$ interactions. Finally, Lanskoy gives in [5] three sets, SLL1, SLL2, SLL3, for the $\Lambda\Lambda$ interaction, or we can switch it off.

The parametrization of Lanskoy and Yamamoto [4] was extracted from G-matrix calculations [20] performed with the Jülich and Nijmegen potentials and were tested on hypernuclei. Other $N\Lambda$ and $\Lambda\Lambda$ interactions were fitted directly to hypernuclei data. The values given by Lanskoy and Yamamoto [4] assume that the nucleon sector is parametrized by the SkM* or SIII interactions while the parameter set of the Salamanca group [6] was used together with the SkS3 interaction. Even though this is

Table 1. Skyrme parameters for the NN interaction (t_0 is given in MeV fm^3, t_1 and t_2 in MeV fm^5, t_3 in MeV fm$^{3+3\alpha}$; the other parameters are adimensional).

Model	α	t_0	t_1	t_2	t_3	x_0	x_1	x_2	x_3
SLy10	1/6	2506.77	430.98	−304.95	13826.41	1.0398	−0.6745	−1.0	1.6833
SkI3	1/4	−1762.88	561.608	−227.09	8106.2	0.3083	−1.1722	−1.0907	1.2926
SkI5	1/4	−1772.91	550.84	−126.685	8206.25	−0.1171	−1.3088	−1.0487	0.3410
SV	1	−1248.3	970.6	107.2	0.	−0.17	0.	0.	1.

Table 2. Skyrme parameters for the $N\Lambda$ interaction [4,19] (u_0 is given in MeV fm^3, u_1 and u_2 in MeV fm^5, u_3 in MeV fm$^{3+3\beta}$, the other parameters are adimensional. V_Λ is the potential felt by a Λ-hyperon in nuclear matter at saturation and is given in MeV.).

Model	β	u_0	u_1	u_2	u_3	y_0	y_3	V_Λ
LY-I	1/3	−476.	42.	23.	1514.1	−0.0452	−0.280	−27.62
LY-IV	1/3	−542.5	56.0	8.0	1387.9	−0.1534	0.1074	−28.17
YBZ-1	1	−349.0	67.61	37.39	2000.	−0.108	0.	−26.52
YBZ-5	1	−315.3	23.14	−23.14	2000	−0.109	0.	−28.50
YBZ-6	1	−372.2	100.4	79.60	2000.	−0.107	0.	−24.98
SkSH1	–	−176.5	−35.8	44.1	0	0	–	−27.68

not fully consistent, we also used other more modern parametrizations in the nucleon sector like the Skyrme Lyon sets [1] in order to investigate the role of the ferromagnetic transition (see sect. 4).

Selected values of the parameter sets are listed in tables 1, 2 and 3. For other parametrizations we refer the reader to the exhaustive table published by Rikovska Stone *et al.* in the case of the NN forces and the papers of Lanskoy *et al.* and Fernandez *et al.* for the $N\Lambda$ and $\Lambda\Lambda$ forces.

As this model only includes the Λ-hyperon, it appears to be less complete than the model of Balberg and Gal [2] which includes all the hyperons. As mentioned in the introduction, we fixed our choice on the parametrization by Lanskoy *et al.* because these authors provide the two-particle potential rather than only the unpolarized energy density. This leaves open the possibility of going beyond the Hartree-Fock approximation and to investigate the response functions of the matter at the RPA level.

It would be straightforward to extend the model to take into account other hyperons such as the Σ^-. Data about the Σ^- in nuclear matter however is rather scarce and the author is not aware of an equivalent Skyrme parametrization including the Σ at the same level of precision. One possibility would be to adjust Skyrme parameters to reproduce Brueckner calculations, *e.g.*, using density matrix expansion techniques. Indeed some data is available from the work of Dabrowski [21], who extracts the potential felt by a Σ^- impurity in nuclear matter at saturation density from Brueckner calculations performed with the Nijmegen potentials. On the other hand, the neglect of the Σ-hyperon is sometimes justified from the very lack of observation of Σ hypernuclei, where this fact is interpreted as indicating that the Σ-nucleon force is in fact repulsive. In that case, β-equilibrium equations would predict that the threshold for Σ-hyperon formation in neutron stars is shifted to very large densities (see, *e.g.*, [2, 21–23]).

Table 3. Skyrme parameters for the $\Lambda\Lambda$ interaction [5] (λ_0 is given in MeV fm^3 and λ_1 in MeV fm^5).

Model	λ_0	λ_1
SLL1	−312.6	57.5
SLL2	−437.7	240.7
SLL3	−831.8	922.9

We will use the model of Balberg and Gal [2] and another by Banik and Bandyopadhyay [24], as well as a simple extrapolation and parametrization of the results of Dabrowski [21], in order to estimate the error committed by neglecting other hyperons and in particular the Σ^-. The results are reported in sect. 6.

3 Threshold for hyperon formation

In neutron star matter we impose that the conditions for β equilibrium are fulfilled. The neutron, proton and Lambda hyperons are subject to the processes

$$p + e^- \rightarrow n + \nu_e\,; \qquad p + e^- \rightarrow \Lambda + \nu_e$$

as well as their inverse

$$n \rightarrow p + e^- + \overline{\nu}_e\,; \qquad \Lambda \rightarrow p + e^- + \overline{\nu}_e\,. \tag{5}$$

We write the equality of the chemical potentials

$$\begin{aligned} &\hat{\mu} = (\mu_n + m_n) - (\mu_p + m_p) = \mu_e - \mu_\nu\,; \\ &\mu_n + m_n = \mu_\Lambda + m_\Lambda\,. \end{aligned} \tag{6}$$

We must also impose electric charge conservation,

$$n_e = n_p\,. \tag{7}$$

At a given baryonic density the electron, proton and hyperon fractions are determined by the solution of eqs. (6),

(7). The chemical potentials are determined by deriving the Skyrme energy density functional with respect to the density of the corresponding particle. Their explicit expression is given in the appendix. The electrons are relativistic and their chemical potential is given by $\mu_e = \sqrt{k_{Fe}^2 + m_e^2}$. In protoneutron star matter with trapped neutrinos we have $\mu_\nu = (6\pi^2 n_\nu)^{(1/3)}$, while in colder neutrino-free neutron star matter, $\mu_\nu = 0$.

The equations should actually take into account the muons in the equation for charge conservation together with the condition $\mu_e = \mu_\mu$. The muons appear namely around saturation density. The muons were neglected in this simplified model. Their effect is in fact not very important, especially in our case where the charged Σ^- is also absent from the model. A sample of the results obtained when taking the muons into account is given in sect. 6.

The threshold for Λ-hyperon formation is determined by the condition

$$\begin{aligned}\mu_\Lambda(\mathrm{thr}) &= \mu_\Lambda(k_{F\Lambda}=0) = \mu_n + m_n - m_\Lambda \\ &= u_0\left(1+\frac{y_0}{2}\right)\rho_N + \frac{3}{8}u_3\left(1+\frac{y_3}{2}\right)\rho_N^{\beta+1} \\ &\quad + \frac{1}{8}\left[u_1(2+y_1)+u_2(2+y_2)\right]k\rho_N^{5/3}\,, \end{aligned} \tag{8}$$

with $k = (3/5)\,(3\pi^2)^{(2/3)}$. It depends on the strength of the ΛN force through the parameters $u_0, u_1, u_2, u_3, \ldots$ and indirectly on the NN force through the chemical potential of the neutron (taken in npe matter in β equilibrium) and is independent of the $\Lambda\Lambda$ force. Depending on the choice of the parameters it is found that the threshold generally occurs between 1.7 $n_{\rm sat}$ and 4 $n_{\rm sat}$ in agreement with other Brueckner-Hartree-Fock or relativistic mean-field calculations. When numerical values are inserted, one can see that the value of $\mu_\Lambda(\mathrm{thr})$ is the result of a delicate cancellation between the u_0 and u_3 terms, the contribution of the u_1, u_2 term being of the order of the sum of the u_0 and u_3 terms. For example, at $\rho_N = 3\ n_{\rm sat}$ and $n_{\rm sat} = 0.16$ fm^{-3} we have for the LY-I parametrization of the $N\Lambda$ force

$$\begin{aligned} &u_0\left(1+\frac{y_0}{2}\right)\rho_N = -223.32\ \mathrm{MeV}\,, \\ &\frac{3}{8}u_3\left(1+\frac{y_3}{2}\right)\rho_N^{\beta+1} = 183.51\ \mathrm{MeV}\,, \\ &\frac{1}{8}\left[u_1(2+y_1)+u_2(2+y_2)\right]k\rho_N^{5/3} = 27.46\ \mathrm{MeV}\,. \end{aligned}$$

Let us also note that the value of $\mu_\Lambda(k_{F\Lambda}=0)$ at saturation density with equal number of neutron and protons is nothing but the single particle potential felt by a Λ impurity in nuclear matter, *i.e.* it should be equal to the binding potential $V_\Lambda \simeq -28$ MeV obtained from data on hypernuclei. The actual values of $V_\Lambda = \mu_\Lambda(k_{F\Lambda}=0, nB = 0.16\ \mathrm{fm}^{-3})$ are reported in the last column of table 2.

We may conclude this section by stating that, once the parametrization of the $N\Lambda$ force has been chosen so that the potential felt by a Λ in nuclear matter reproduces the experimental value, the condition that the threshold density for Λ-hyperons in nuclear matter in β equilibrium should lay around 2-3 times saturation density does not severely constrain the admissible Skyrme NN and $N\Lambda$ forces. We observe that stiffer equations of state (eos) and the eos allowing for a larger proton fraction have lower hyperon thresholds (see table 5 for a sample of the results).

4 Transition to ferromagnetic state

4.1 Criterion for a ferromagnetic instability

Previous studies on the neutrino mean free path in neutron matter [9] or npe^- matter in β equilibrium [11] found that a pole appears in the calculation of the axial structure function above a certain critical density. This feature is typical of Skyrme models and is related to a transition to a ferromagnetic state. In this section we will study how this critical density is affected by the presence of hyperons.

Let us define the magnetic susceptibilities χ_{ij} where $i, j \in \{n, p, \Lambda\}$:

$$\frac{1}{\chi_{ij}} = \frac{\partial^2 \mathcal{E}}{\partial \mathcal{M}_i \partial \mathcal{M}_j}\,, \qquad \mathcal{M}_i = \kappa_i(\rho_{i\uparrow} - \rho_{i\downarrow})\,, \tag{9}$$

where $\mathcal{E} = \mathcal{E}(\rho_{n\uparrow}, \rho_{n\downarrow}, \rho_{p\uparrow}, \rho_{p\downarrow}, \rho_{\Lambda\uparrow}, \rho_{\Lambda\downarrow})$ is the polarized energy density functional, $\mathcal{M}_i$ are the magnetizations and κ_i are the magnetic moments. The inverse susceptibilities are therefore proportional to the second derivatives of the energy density functional with respect to the polarizations:

$$\begin{aligned} &\frac{\kappa_i\kappa_j}{\chi_{ij}} = \frac{2\rho}{\rho_i\rho_j}\Delta_{ij}\,, \\ &\Delta_{ij} = \frac{1}{2}\frac{\partial^2(\mathcal{E}/\rho)}{\partial s_i \partial s_j} \quad \text{with} \quad s_i = \frac{\rho_{i\uparrow}-\rho_{i\downarrow}}{\rho_{i\uparrow}+\rho_{i\downarrow}}\,. \end{aligned} \tag{10}$$

On the other hand, it can be shown that the Δ_{ij} are related to the Landau parameters g_0^{ij} defined in the appendix through

$$\begin{aligned} &\Delta_{ij} = \frac{2\rho}{\rho_i\rho_j}\frac{1}{\sqrt{N_0^i N_0^j}}G_0^{ij}\,, \quad \text{if } i \neq j\,, \\ &\Delta_{ii} = \frac{2\rho}{\rho_i^2}\frac{1}{N_0^i}(1+G_0^{ii})\,, \\ &G_0^{ij} = \sqrt{N_0^i N_0^j}\,g_0^{ij}\,, \qquad N_0^i = \frac{m_i^* k_{Fi}}{\pi^2\hbar^2}\,. \end{aligned} \tag{11}$$

A criterion for the appearance of the ferromagnetic phase is that the determinant of the inverse susceptibility matrix vanishes,

$$\mathrm{Det}\begin{pmatrix} 1/\chi_{nn} & 1/\chi_{np} & 1/\chi_{n\Lambda} \\ 1/\chi_{pn} & 1/\chi_{pp} & 1/\chi_{p\Lambda} \\ 1/\chi_{\Lambda n} & 1/\chi_{\Lambda p} & 1/\chi_{\Lambda\Lambda} \end{pmatrix} = 0 \tag{12}$$

and in terms of the Landau parameters:

$$\mathrm{Det}\begin{pmatrix} (1+G_0^{nn}) & G_0^{np} & G_0^{n\Lambda} \\ G_0^{pn} & (1+G_0^{pp}) & G_0^{p\Lambda} \\ G_0^{\Lambda n} & G_0^{p\Lambda} & (1+G_0^{\Lambda\Lambda}) \end{pmatrix} = 0\,. \tag{13}$$

It can be shown that this quantity appears in the denominator of the static axial response (see [16]).

4.2 Dependence of the criterion on parameter sets

A few NN forces (MSk7, SkX, SkS3) had to be discarded as not convenient for obtaining the equation of state away from saturation, some more for not permitting the formation of hyperons below 5 $n_{\rm sat}$, others again for undergoing a transition to pure neutron matter before the threshold for hyperon formation was reached (SIII, SI′, SIII′, Skz0–Skz4).

The remaining ones all display a transition to the ferromagnetic state at some critical density $n_{\rm ferro}^{\beta-npe}$ when no hyperons are present, with the exception of the SV force. Usually, the ferromagnetic transition occurs earlier in pure neutron matter (PNM) than in symmetric nuclear matter (SNM), and at an intermediate density for npe matter in β equilibrium. One exception is the case of the Lyon Skyrme forces where the reverse situation appears to occur. A closer look nevertheless reveals that only traces of protons are enough to drastically lower the critical density in very neutron-rich matter so that the usual pattern is in fact recovered.

Some forces (SkO, SkO′, SkI1, SkI4, SkT4, SkT5) again need to be discarded since the ferromagnetic transition occurs below $n_{\rm sat}$ in symmetric nuclear matter, so that the nuclei would in fact be unstable with respect to spin fluctuations. This leaves us with forces for which the $n_{\rm ferro}^{\beta-npe}$ occurs in the range $n_{\rm sat}$–3 $n_{\rm sat}$, and the threshold for Λ-hyperon formation in the range 1.7 $n_{\rm sat}$–4 $n_{\rm sat}$. A key point is now whether $n_{\rm ferro}^{\beta-npe}$ is greater or lower than $n_{\rm thr}^{\Lambda}$. While the criterion for the onset of the ferromagnetic instability eq. (13) decreases with increasing density in npe matter in β equilibrium, we noted that it always tends to increase again when enough hyperons are present. This then rejects the critical density $n_{\rm ferro}^{\beta-npe\Lambda}$ for the onset of ferromagnetism in $np\Lambda e$ matter in β equilibrium to higher densities. In a few cases the instability even disappears altogether. For the majority of NN parameter sets, the ferromagnetic transition occurs before the threshold for hyperon formation. In some cases (SLy4, SLy7, SGI), we have $n_{\rm thr}^{\Lambda} \sim< n_{\rm ferro}^{\beta-npe}$, and the ferromagnetic transition is only delayed by a tiny amount.

We finally selected four NN forces (SLy10, SkI3, SkI5, SV) as relevant for our purpose, namely to study neutron star matter with a hyperonic component before the ferromagnetic transition sets in. In fig. 1 (top, middle, bottom) we have represented the criterion (13) for these parametrizations of the NN Skyrme force and various choices of the $N\Lambda$ and $\Lambda\Lambda$ forces. The modification of the slope at the hyperon threshold around 2 $n_{\rm sat}$ is clearly visible in fig. 1.

The SV NN interaction is atypical as it has no t_3-term. This parametrization is especially interesting since, among all tested NN interactions, it was the only one which does not give a ferromagnetic instability in npe matter in β equilibrium. This parametrization is rather old (1975) but yields an acceptable description of the properties of nuclear matter and nuclei and it complies with all the conditions necessary for describing a viable neutron star. The SLy10, SkI3 and SkI5 are modern forces. The SLy10 set

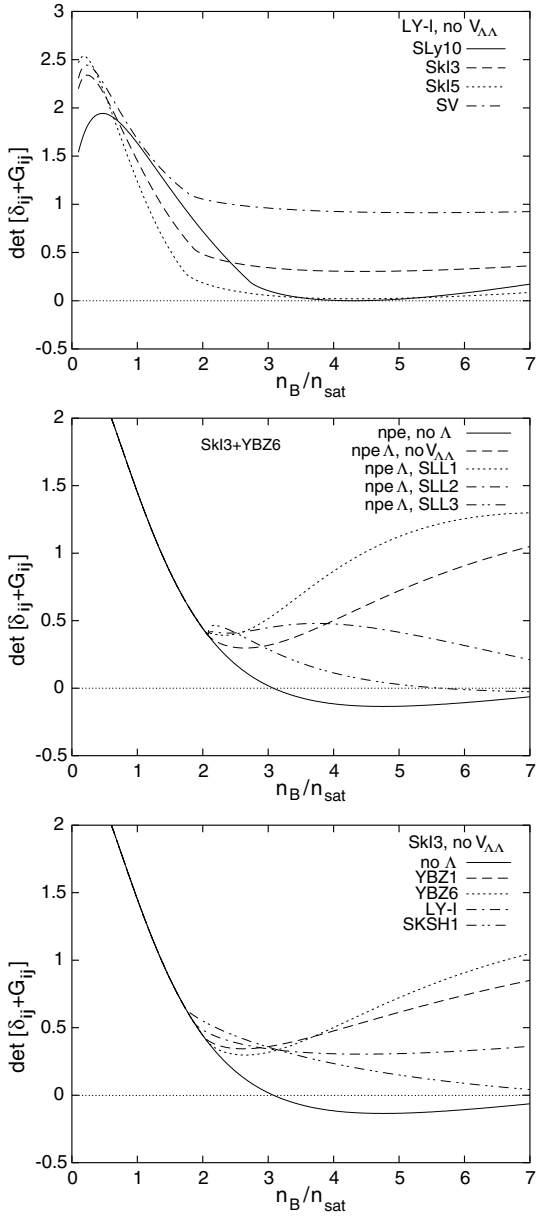

Fig. 1. Criterion for the transition to a ferromagnetic state as a function of density, displaying the influence of the choice of interactions: choice of the NN force (top panel), of the $N\Lambda$ force (middle panel) and of the $\Lambda\Lambda$ force (lower panel).

was designed to reproduce features of pure neutron matter as obtained from the variational calculations of Wiringa *et al.* in view of its application to neutron stars. The SkI3 and SkI5 sets were designed in order to improve isotope shifts and incorporate the dipole sum rule enhancement factor $\kappa = 0.25$. Let us notice that the SkI3, SkI5 and SV allow for larger proton fractions than the SLy10, in particular we can see from table 4 that the criterion for opening of the direct URCA process with nucleons is reached before the theshold for hyperon production.

The behaviour of the criterion for ferromagnetic instability is qualitatively very similar for all choices of the $N\Lambda$ interaction. Forces yielding smaller ρ_Λ(thr) and softer eos

Table 4. a)-d): thresholds for ferromagnetism in $npΛe$ matter in β equilibrium.

a) NN force = SLy10 (threshold for ferromagnetism in PNM: 3.837 $n_{\rm sat}$, in SNM: 3.821 $n_{\rm sat}$, in npe matter in β equilibrium: 3.055 $n_{\rm sat}$).

$N\Lambda$	$n_{\rm thr}$	Y_p	no $\Lambda\Lambda$	SLL1	SLL2	SLL3
LY-I	2.719	0.041	grazing [4.3]	no pole	6.183	3.898
LY-II	2.868	0.040	3.160	3.212	3.236	3.328
LY-IV	2.764	0.041	3.657	no pole	6.480	3.818
YBZ5	3.319	0.037	–	–	–	–
YBZ6	5.101	0.029	–	–	–	–
SKSH1	2.294	0.044	4.577	5.297	4.729	4.153

b) NN force = SkI3 (threshold for ferromagnetism in PNM: 2.298 $n_{\rm sat}$, in SNM: 5.73 $n_{\rm sat}$, in npe matter in β equilibrium: 3.078 $n_{\rm sat}$).

$N\Lambda$	$n_{\rm thr}$	Y_p	no $\Lambda\Lambda$	SLL1	SLL2	SLL3
LY-I	1.864	0.126	no pole	no pole	9.234	4.663
LY-IV	1.873	0.127	no pole	no pole	8.900	4.548
YBZ1	2.015	0.139	no pole	no pole	8.753	4.893
YBZ5	1.942	0.133	no pole	no pole	7.550	4.080
YBZ6	2.076	0.144	no pole	no pole	9.194	5.633
SKSH1	1.739	0.116	8.225	9.495	6.765	4.425
SKSH2	1.681	0.111	18.875	15.250	8.253	4.212

c) NN force = SkI5 (threshold for ferromagnetism in PNM: 1.772 $n_{\rm sat}$, in SNM: 2.659 $n_{\rm sat}$, in npe matter in β equilibrium: 2.140 $n_{\rm sat}$).

$N\Lambda$	$n_{\rm thr}$	Y_p	no $\Lambda\Lambda$	SLL1	SLL2	SLL3
LY-I	1.727	0.150	grazing [4.34]	no pole	4.707	3.166
LY-IV	1.734	0.150	grazing [4.14]	no pole	4.627	3.095
YBZ1	1.838	0.162	no pole	no pole	8.656	3.622
YBZ5	1.785	0.156	no pole	no pole	5.404	3.239
YBZ6	1.882	0.167	no pole	no pole	9.118	3.950
SKSH1	1.629	0.138	3.337	3.914	3.541	3.103

d) NN force = SV (threshold for ferromagnetism in PNM: 4.850 $n_{\rm sat}$, in SNM: no pole, in npe matter in β equilibrium: no pole).

$N\Lambda$	$n_{\rm thr}$	Y_p	no $\Lambda\Lambda$	SLL1	SLL2	SLL3
LY-I	1.793	0.125	no pole	no pole	9.330	4.576
LY-IV	1.800	0.126	no pole	no pole	9.143	4.533
YBZ1	1.906	0.133	no pole	no pole	8.649	4.635
YBZ3	1.672	0.116	no pole	no pole	11.700	5.050
YBZ5	1.851	0.129	no pole	no pole	7.521	3.956
YBZ6	1.951	0.136	no pole	no pole	9.093	5.200
SKSH1	1.691	0.118	no pole	no pole	8.920	4.250
SKSH2	1.635	0.114	no pole	no pole	8.253	4.068

(see sect. 5) also tend to be more efficient in lifting the ferromagnetic criterion $\det[\delta_{ij} + G_{ij}]$ above the critical zero axis. This is especially the case for the $YBZ4$ parameter set which permitted to avoid the pole also in the SLy4 and SLy7 parametrizations of the NN force. However the YBZ4 parameter set was rejected by Lanskoy on the ground that it gives overbinding of the Λ in hypernuclei so that we will not consider it further. Despite this overall similarity the actual presence and position of the pole is sensitive to the choice of the $N\Lambda$ force. This happens because the $\det[\delta_{ij} + G_{ij}]$ has already decreased considerably prior to ρ_Λ(thr) and the turnover due to the contribution of the Λ therefore must take place in the vicinity of the zero axis.

We can also see on this figure that the $\Lambda\Lambda$ interaction plays an important role in determining $n_{\rm ferro}^{\beta-npe\Lambda}$. The set SLL3 (which also gives a stiffer eos, see next section) is less efficient in removing the pole while the SLL1 set which gives the softest eos is also the most efficient in preventing the onset of ferromagnetism. The $\Lambda\Lambda$ force of Lanskoy [5] is very schematic (it is parametrized by λ_0 and λ_1 only, see the appendix); moreover, it was adjusted

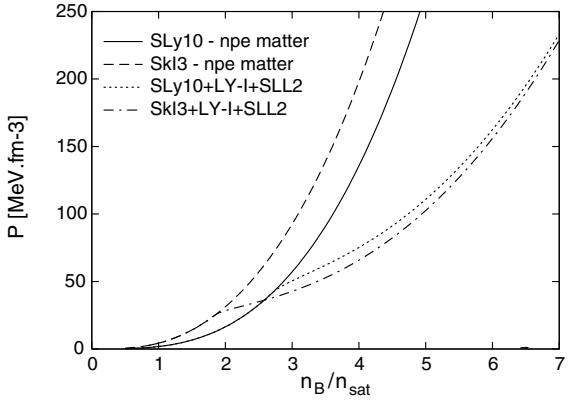

Fig. 2. Typical results for the equation of state.

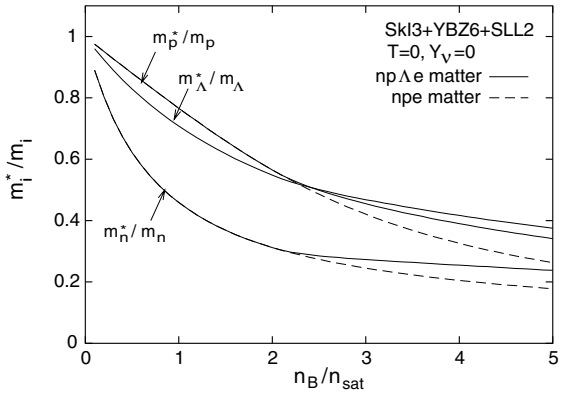

Fig. 3. Modification of the effective masses by the presence of hyperons.

to the older value $\Delta B_{\Lambda\Lambda} = -4.8$ MeV instead of the value $\Delta B_{\Lambda\Lambda} \simeq -1$ MeV recently extracted from the "Nagara event". The case where a vanishing $\Lambda\Lambda$ interaction is assumed may in fact be closer to the true situation. A better knowledge of the $\Lambda\Lambda$ interaction at high density is needed.

The values of density and proton content at the threshold for hyperon formation as well as the critical values for the ferromagnetic transition for various models are gathered in table 4 a)-d). All densities are quoted in units of the saturation density of the corresponding model. The mention "grazing" means that $\det[\delta_{ij} + G_{ij}]$, while not actually crossing the zero axis, comes so near it that for all practical purposes the static axial response function will behave as if a pole were present.

5 Equation of state and neutron star structure

5.1 Equation of state, effective masses and the hyperon fraction

For neutron star matter in β equilibrium without hyperons, the equations of state are in order of decreasing stiffness parametrized by the NN interaction SV > SkI3, SkI5 > SLy10. The parametrizations SkI3 and SkI5 yield nearly indistinguishable results, so that SkI5 will not be considered further in the remainder of this work. When the hyperons are taken into account in the calculation of the β equilibrium, the equation of state softens as expected. For a given NN interaction, we have, in order of decreasing stiffness, YBZ6 > YBZ1 > LY-I, LY-IV > YBZ3 > SKSH2 > SKSH1. Finally, when varying the $\Lambda\Lambda$ interaction for given NN and $N\Lambda$ forces, we obtain SLL3 > SLL2 > SLL1. If the $\Lambda\Lambda$ interaction is set to zero, the equation of state is somewhat stiffer than SLL2 at $n_B < 5\ n_{\rm sat}$ and much softer above $5\ n_{\rm sat}$. We note the sizable effect of the $\Lambda\Lambda$ interaction on the equation of state, as well as in the previous section on the value of the Landau parameters.

The equation of state is shown in fig. 2 for two of our preferred NN forces, and with the same choice LY-I for the $N\Lambda$ interaction and SLL2 for the $\Lambda\Lambda$ interaction. Even though SkI3 was stiffer than SLy10 without hyperons, the combination SkI3 + LYI + SLL2 gives rise to a higher hyperon content at a given density (see also fig. 4) than SLy10 + LYI + SLL2, so that it is also subject to more softening. As a consequence, the eos with hyperons are very similar.

Figure 3 illustrates the behavior of the effective masses in the case of the parameter set SkI3 + YBZ6 + SLL2. The effective masses of the neutrons are lower than that of protons in neutron-rich matter, a feature generally encountered in Skyrme models. The presence of hyperons causes both the neutron and proton mass to decrease less rapidly at high density.

Figure 4 shows the particle fractions $Y_i = n_i/n_B$ as a function of total baryonic density n_B for the SkI3 + YBZ6 + SLL2 and SLy10 + LYI + SLL2 parameter sets. It can be seen in the top panel that the hyperons appear at higher density and are less numerous for a given density with SLy10 + LYI + SLL2 than with SkI3 + YBZ6 + SLL2. The bottom panel shows the chemical composition of matter with a non-vanishing number of trapped neutrinos at zero temperature. The case with trapped neutrinos and finite temperature relevant for protoneutron stars will be discussed further in sect. 7.

5.2 Solution of the Tolman-Oppenheimer-Volkoff equation

Our selected parameter sets still have to pass the test of causality in the density range of interest, and whether they can support neutron stars with maximum masses larger than the observed value 1.4 $M_\odot$.

The properties of neutron stars formed of *npe* matter in β equilibrium were calculated by Rikovska Stone *et al.* [3] for a large number of Skyrme parametrizations. The four NN interactions that we singled out in sect. 4 all belong to the subset of interactions selected by these authors as giving viable neutron stars, with maximum masses of the order 2 $M_\odot$ to 2.4 $M_\odot$. The central density reached in stars with the maximum mass is slightly larger than the density at which the velocity of sound reaches the velocity of light for the SLy10 and SV parametrizations whereas

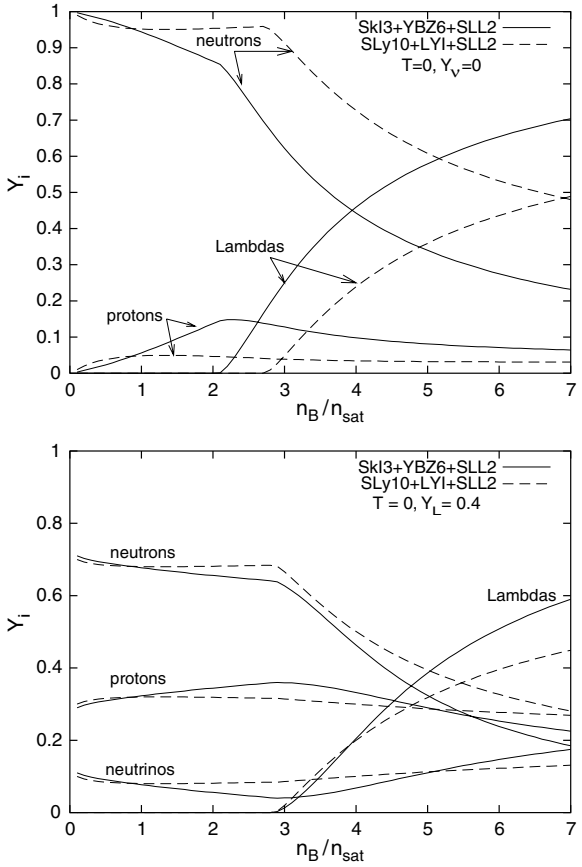

Fig. 4. Particle fractions from the SkI3 + YBZ6 + SLL2 and SLy10 + LYI + SLL2 parametrizations. Top: in neutrino-free matter; bottom: with trapped neutrinos and lepton fraction $Y_L = 0.4$.

the equation of state obtained with SkI3 and SkI5 always remains causal. In any case, stars with the fiducial mass 1.4 $M_\odot$ always fulfill $n_c(1.4\ M_\odot) < n_B(c_s^2 = 1)$.

When hyperons are added, the equation of state being softer, the limit $c_s^2 = 1$ is reached for larger densities. It is pushed to $\sim$ 8–11 times saturation density for the SLL3 parametrization of the $\Lambda\Lambda$ interaction, to $\sim$ 13–16 $n_{\rm sat}$ for the SLL2 parametrization and is larger than 20 $n_{\rm sat}$ for the SLL1 set. The case where a vanishing $\Lambda\Lambda$ interaction is assumed always remains causal. In any case, such densities are beyond the range of validity of the model. As a consequence, although the softening of the eos with hyperons gives rise to higher compression rates and larger central densities in neutron stars than in stars made of *npe* matter only, the criterion $c_s^2 < 1$ is always fulfilled up to the central density of the most massive stars in our neutron star models with hyperons, except a few instances involving the SLL3 parameter set.

We have solved the Tolman-Oppenheimer-Volkoff equation to obtain the (non-rotating) neutron star mass-radius relation. The equation of state is matched at lower densities with that of Negele and Vautherin [25] for $\rho \in [0.001-0.08]$ fm^{-3} and with the Baym-Pethick-Sutherland (BPS) [26] equation of state for $\rho < 0.001$ fm^{-3}. The results[1] are summarized in table 5 a)-d) and a sample of mass-radius curves is shown in figs. 5 and 6. For each combination of the NN, $N\Lambda$ and $\Lambda\Lambda$ interaction we give the density at which the speed of sound becomes superluminal, the central density and radius of a 1.4 $M_\odot$ in case it can be formed, and the central density and radius of the star with maximum mass $M_{\rm max}$.

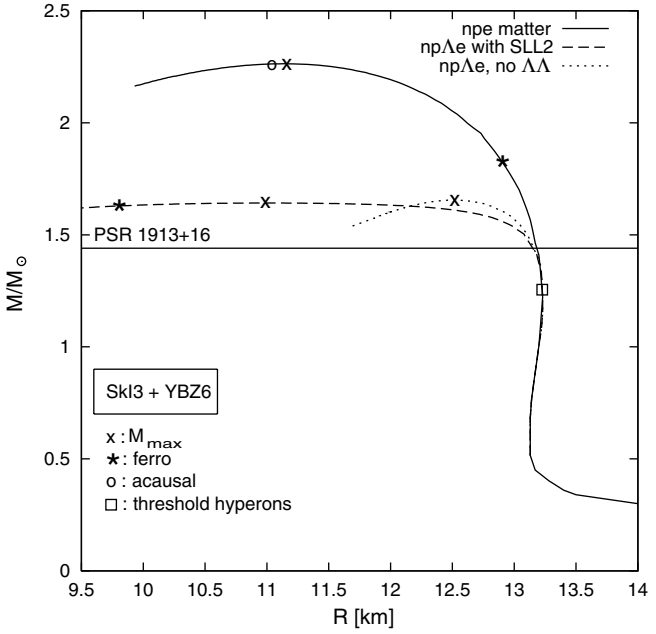

Fig. 5. Neutron star mass-radius relation with the Skyrme SkI3 + YBZ6 interaction, with and without hyperons.

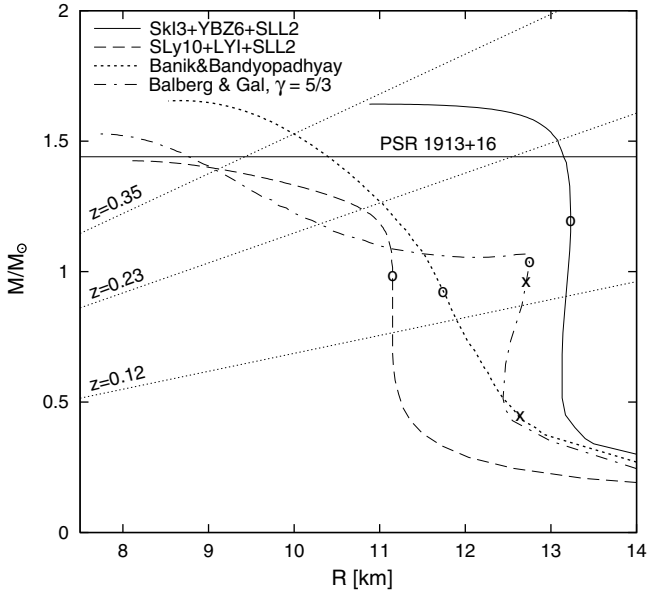

Fig. 6. Neutron star mass-radius relation for several non-relativistic models of baryonic matter.

[1] The parameters we obtained for the stars composed of *npe* matter may differ very slightly from those quoted by Rikovska Stone *et al.*, presumably due to a different matching at low density or the neglect of the muons.

Table 5. Conditions for causality and neutron star properties.

a) NN force = SLy10 (in *npe* matter in β equilibrium: $n_B(c_s^2{=}1){=}7.308$ $n_{\rm sat}$, $n_c(1.4\ M_\odot){=}3.60$ $n_{\rm sat}$, $R(1.4\ M_\odot){=}11.05$ km, $n_{\rm max} = 7.69$ $n_{\rm sat}$, $M_{\rm max} = 1.99$ $M_\odot$, $R(M_{\rm max}) = 9.52$ km).

$N\Lambda$	$\Lambda\Lambda$	$n_B(c_s^2 = 1)$	$n_c(1.4\ M_\odot)$	$R(1.4\ M_\odot)$	$n_{\rm max}$	$M_{\rm max}$	$R(M_{\rm max})$
LY-I	no $\Lambda\Lambda$	causal	–	–	6.94	1.317	10.36
LY-I	SLL1	> 20	–	–	5.99	1.210	10.70
LY-I	SLL2	16.032	9.38	9.0	12.38	1.425	8.11
LY-I	SLL3	11.036	5.25	10.42	10.23	1.658	8.55
LY-IV	no $\Lambda\Lambda$	causal	–	–	6.82	1.338	10.43
LY-IV	SLL2	15.880	8.49	9.35	12.07	1.437	8.21
SKSH1	no $\Lambda\Lambda$	> 20	–	–	5.09	0.875	10.8
SKSH1	SLL2	> 20	–	–	20.6	1.159	6.19
SKSH1	SLL3	13.210	10.25	8.15	13.65	1.453	7.40
YBZ5	no $\Lambda\Lambda$	causal	–	–	5.51	1.377	10.98
YBZ5	SLL1	> 20	–	–	4.94	1.234	11.11
YBZ5	SLL2	13.825	7.11	10.04	11.64	1.456	8.34
YBZ5	SLL3	8.440	4.14	10.97	9.41	1.789	8.92

b) NN force = SkI3 (in *npe* matter in β equilibrium: $n_B(c_s^2 = 1) = 6.343$ $n_{\rm sat}$, $n_c(1.4\ M_\odot){=}2.27$ $n_{\rm sat}$, $R(1.4\ M_\odot) = 13.21$ km, $n_{\rm max} = 6.12$ $n_{\rm sat}$, $M_{\rm max} = 2.263$ $M_\odot$, $R(M_{\rm max}) = 11.16$ km).

$N\Lambda$	$\Lambda\Lambda$	$n_B(c_s^2 = 1)$	$n_c(1.4\ M_\odot)$	$R(1.4\ M_\odot)$	$n_{\rm max}$	$M_{\rm max}$	$R(M_{\rm max})$
LY-I	no $\Lambda\Lambda$	causal	–	–	4.34	1.339	12.57
LY-I	SLL1	> 20	–	–	3.71	1.263	12.98
LY-I	SLL2	15.880	10.44	8.99	12.59	1.413	8.30
LY-I	SLL3	10.514	3.96	12.24	9.50	1.723	9.19
LY-IV	no $\Lambda\Lambda$	causal	–	–	4.33	1.351	12.68
LY-IV	SLL2	15.739	9.59	9.34	12.44	1.422	8.35
LY-IV	SLL3	10.400	3.83	12.37	9.36	1.734	9.25
YBZ1	no $\Lambda\Lambda$	causal	2.52	13.20	4.49	1.534	12.59
YBZ1	SLL2	13.293	2.75	13.13	9.53	1.545	9.51
YBZ1	SLL3	7.764	2.68	13.17	7.93	1.907	9.85
YBZ5	SLL2	13.969	9.57	9.27	12.56	1.427	8.22
YBZ5	SLL3	8.269	3.43	12.69	8.74	1.822	9.37
YBZ6	no $\Lambda\Lambda$	causal	2.36	13.20	4.66	1.655	12.52
YBZ6	SLL1	> 20	2.38	13.19	4.12	1.553	12.82
YBZ6	SLL2	13.077	2.39	13.19	6.79	1.642	11.02
YBZ6	SLL3	7.439	2.41	13.18	7.43	1.967	10.16
SKSH1	no $\Lambda\Lambda$	> 20	–	–	3.32	1.116	13.02
SKSH1	SLL2	> 20	–	–	3.07	1.073	13.11
SKSH1	SLL3	12.46	7.25	9.91	12.08	1.544	8.20
SKSH2	SLL2	15.497	–	–	3.16	1.041	13.0
SKSH2	SLL3	9.971	5.81	10.55	10.83	1.658	8.46

c) NN force = SkI5 (in *npe* matter in β equilibrium: $n_B(c_s^2 = 1) = 6.377$ $n_{\rm sat}$, $n_c(1.4\ M_\odot) = 2.10$ $n_{\rm sat}$, $R(1.4\ M_\odot){=}13.87$ km, $n_{\rm max} = 6.08$ $n_{\rm sat}$, $M_{\rm max} = 2.273$ $M_\odot$, $R(M_{\rm max}) = 11.36$ km).

$N\Lambda$	$\Lambda\Lambda$	$n_B(c_s^2 = 1)$	$n_c(1.4\ M_\odot)$	$R(1.4\ M_\odot)$	$n_{\rm max}$	$M_{\rm max}$	$R(M_{\rm max})$
LY-I	SLL2	15.915	–	–	3.70	1.297	13.32
LY-I	SLL3	10.544	3.84	12.77	9.52	1.719	9.27
YBZ6	no $\Lambda\Lambda$	causal	2.20	13.85	4.44	1.627	12.96
YBZ6	SLL2	13.103	2.25	13.84	7.64	1.615	10.65
YBZ6	SLL3	7.470	2.28	13.85	7.48	1.958	10.22
SKSH1	SLL2	> 20	–	–	2.80	1.133	13.85
SKSH1	SLL3	12.494	7.28	10.08	12.09	1.541	8.26

Table 5. Continued.

d) NN force = SV (in npe matter in β equilibrium: $n_B(c_s^2 = 1) = 4.983$ $n_{\rm sat}$, $n_c(1.4\ M_\odot) = 2.10$ $n_{\rm sat}$, $R(1.4\ M_\odot) = 13.46$ km, $n_{\rm max} = 5.44$ $n_{\rm sat}$, $M_{\rm max} = 2.426$ $M_\odot$, $R(M_{\rm max}) = 11.54$ km).

$N\Lambda$	$\Lambda\Lambda$	$n_{c_s^2=1}$	$n_c(1.4\ M_\odot)$	$R(1.4\ M_\odot)$	$n_{\rm max}$	$M_{\rm max}$	$R(M_{\rm max})$
LY-I	no $\Lambda\Lambda$	causal	–	–	4.08	1.368	12.80
LY-I	SLL1	> 20	–	–	3.53	1.291	13.15
LY-I	SLL2	15.412	9.39	9.44	12.38	1.424	8.37
LY-I	SLL3	9.553	3.54	12.69	9.03	1.768	9.34
LY-IV	no $\Lambda\Lambda$	causal	–	–	4.08	1.379	12.96
LY-IV	SLL2	15.317	8.78	9.73	12.14	1.432	8.45
YBZ1	SLL2	13.291	2.52	13.35	9.57	1.544	9.52
YBZ1	SLL3	7.558	2.49	13.40	7.69	1.925	9.97
YBZ6	no $\Lambda\Lambda$	causal	2.19	13.40	4.44	1.662	12.75
YBZ6	SLL1	> 20	2.21	13.40	4.01	1.562	13.04
YBZ6	SLL2	13.082	2.22	13.41	6.5	1.639	11.24
YBZ6	SLL3	7.253	2.25	13.42	7.24	1.984	10.27
SKSH1	no $\Lambda\Lambda$	> 20	–	–	3.22	1.157	13.17
SKSH1	SLL2	18.318	–	–	3.06	1.111	13.24
SKSH1	SLL3	10.914	6.09	10.54	11.07	1.612	8.44

As a rule of thumb, it is known that the stiffer the equation of state is, the larger will be the maximum mass of the neutron star. Our results for $M_{\rm max}$ follow accordingly to the classification in stiffness given at the beginning of this section. Thus, the SKSH1 choice generally yields $M_{\rm max} < 1.4\ M_\odot$, whereas the YBZ6 always passes this test successfully. We see again that the choice of the $\Lambda\Lambda$ interaction is crucial to determine whether or not the star is able to reach to $1.4\ M_\odot$ line. When the $\Lambda\Lambda$ interaction is switched off or for the SLL1 choice, the equation of state is generally too soft to support a 1.4 neutron star. On the other hand, the SLL3 always succeeds in producing $M_{\rm max} > 1.4\ M_\odot$. The SLL2 choice barely makes it to $1.4\ M_\odot$ for intermediate choices of the $N\Lambda$ interaction. This results in a plateau feature, where tiny additions of mass effect a large reduction of radius without actually reaching the instability, the $M = 1.4\ M_\odot$ point being finally reached at unprobably high densities $\rho > 10\ n_{\rm sat}$ much beyond the validity of the model. A stiff equation of state on the other hand is not convenient, since it favours ferromagnetism to appear earlier. The latter condition usually rules out the SLL3 choice.

For the SLy10 choice of the NN interaction ferromagnetism always sets in before the central density of a $1.4\ M_\odot$ star is reached. In particular, it must be reminded at this point that ferromagnetism is reached before the threshold of production of hyperons for the choices YBZ1, YBZ5, YBZ6. For the SkI3 choice, the criterion $n_c(1.4\ M_\odot) < n_{\rm ferro}$ is satisfied for the sets (SkI3 + LY-IV + SLL3), (SkI3 + YBZ5 + SLL3) and (SkI3 + YBZ1 or YBZ6 + any choice of $\Lambda\Lambda$). The star with the maximum mass also fulfills all requirements if it is described by (SkI3 + YBZ6 + no $\Lambda\Lambda$) or (SkI3 + YBZ6 + SLL2). The results obtained with the choice SkI5 are very similar. The choice SV represents an intermediate situation. The $1.4\ M_\odot$ star fulfills both criteria $n_c(1.4\ M_\odot) < n_B(c_s^2 = 1)$ and $n_c(1.4\ M_\odot) < n_{\rm ferro}$ in the cases (SV + LY-I + SLL3), (SV + LY-IV + SLL2), (SV + YBZ1 + SLL2/3), (SV + YBZ6 + any choice of $\Lambda\Lambda$). Moreover, the star with the maximum mass also fulfills both criteria for the choices (SV + YBZ6 + no $\Lambda\Lambda$) and (SV + YBZ6 + SLL2).

In fig. 6 we compare the mass-radius relation obained in several non-relativistic models of matter in β equilibrium with hyperons. As discussed above, among our Skyrme parametrizations the best are the SkI3 + YBZ6 + SLL2 and the SLy10 + LYI + SLL2 sets. The SkI5 or SV forces again give results very similar to those of the SkI3 force. The maximum mass reached with the stiffer SkI3 + YBZ6 + SLL2 set is $1.64\ M_\odot$ comfortably above the Hulse-Taylor value $1.44\ M_\odot$, while the maximum mass permitted by the softer SLy10 + LYI + SLL2 set, $1.42\ M_\odot$, falls a bit short. This is however not an uncommon feature in non-relativistic models (see Brueckner-Hartree-Fock calculations [27,28]). Among the parametrizations given by Balberg and Gal [2], that with intermediate compressibility corresponding to $\gamma = 5/3$ was chosen. Figure 6 also displays the results obtained with a density-dependent Seyler-Blanchard potential as parametrized by Banik and Bandyopadhyay [24]. In contrast to our Skyrme forces, the models of Balberg and Gal and of Banik and Bandyopadhyay both take into account Σ-hyperons (see table 6). The threshold for hyperon formation is represented in the figure with circles for the Λ and crosses for the Σ.

The parametrization of Balberg and Gal is in fact unstable slightly above the Λ-hyperon threshold. As a consequence, the M *vs.* R relation displays an extended plateau, then recovers, crosses the line $M = 1.4\ M_\odot$ and finally reaches a maximum at $M = 1.53\ M_\odot$.

Also represented in the figure are lines of constant gravitational redshift:

$$z = \left(1 - \frac{2GM}{Rc^2}\right)^{-1/2} - 1\,.$$

Table 6. Neutron star properties for the models of Balberg and Gal [2] and Banik and Bandyopadhyay [24].

Model	$n_{\rm thr}^{\Sigma}$	$n_{\rm thr}^{\Lambda}$	$R(1.4\ M_\odot)$	$n_c(1.4\ M_\odot)$	$M_{\rm max}$	$R(M_{\rm max})$	$n_c(M_{\rm max})$
Balberg $\gamma = 5/3$	1.82	2.32	9.02	8.5	1.53	7.74	12.8
Banik & Bandyo.	1.52	2.82	10.6	5.4	1.66	8.68	10.2

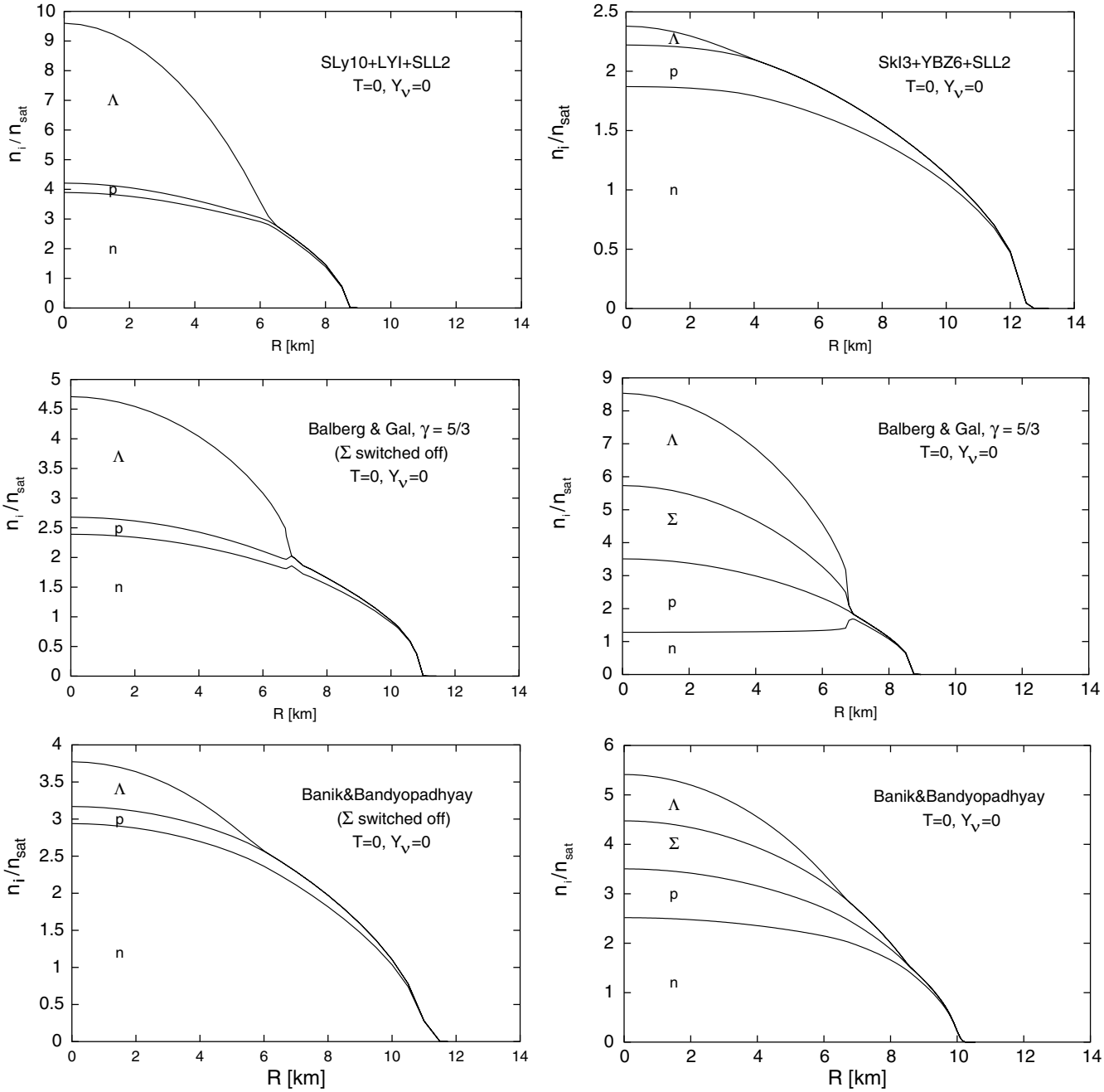

Fig. 7. Density profile of a 1.4 $M_\odot$ neutron star for several non-relativistic models of baryonic matter.

To date, two determinations exist from the observation of spectral lines in isolated neutron stars [29]. Sanwal *et al.* obtained a result with a large error bar, $z = 0.12$–0.23, while Cottam *et al.* could extract a precise determination $z = 0.35$. All the neutron star models displayed would be compatible with the determination of Sanwal *et al.* Almost all models are also in agreement with the value $z = 0.35$ of Cottam *et al.* On the other hand, the mass-radius relation from the SkI3 + YBZ6 + SLL2 set is only marginally compatible with this value.

Figure 7 displays the density profile of a 1.4 $M_\odot$ neutron star and its hyperonic content. The profiles corresponding to two of the Skyrme parameters sets studied in this work, SkI3 + YBZ6 + SLL2 and SLy10 + LYI + SLL2 (top panels) are compared to a version of the models of Balberg and Gal [2] and of Banik and Bandyopadhyay [24]

Table 7. Influence of the muons on the threshold for hyperon production.

	$n_{\rm thr}(\mu)$	$n_{\rm thr}(\Lambda)$	$Y_p^{\rm thr}$
SkI3 + YBZ6 + SLL2	0.782	2.194	0.186
SLy10 + LYI + SLL2	0.721	2.726	0.052
SV + YBZ6 + SLL2	0.752	2.024	0.169

(medium and bottom left panels), where all hyperons save the Λ's are artificially switched off. The profiles corresponding to the latter two models when also Σ^--hyperons are taken into account is displayed on the medium and bottom right panels. We can see that additional hyperons make the equation of state softer and the neutron star more compact.

6 Influence of the neglect of muons or Σ^--hyperons

In this section we will stop for a moment to consider the probable impact on our conclusions of the error committed by neglecting some particles in the model.

Let us first justify the claim made in sect. 3 that we could safely neglect the muons. The threshold for muon production was calculated using our three preferred NN forces SkI3, SLy10 and SV. It is found to lie around three quarters of the saturation density (see table 7). Muons are thus present through all the star except the crust if it is assumed that the star is made of $(np\Lambda e^-\mu^-)$ matter. They are known to disappear at high density if charged hyperons (like the Σ^-) are taken into account. The muon fraction however never comes to be very high, and the respective fractions of n, p and Λ baryons are little altered, as can be seen in fig. 8 (top panel). Since the Landau parameters only depend on the baryonic densities, the ferromagnetic criterion is also not appreciably modified (see fig. 8, central panel). Finally, the contribution to the equation of state is also imperceptible (fig. 8, bottom panel).

Much more severe could be the influence of other hyperons, especially the Σ^-. We have already mentioned in the previous section, and it can be plainly seen in fig. 7 (middle and lower panels), that the effect on the composition, equation of state and neutron star structure is indeed important: as a matter of fact, it is a well-known result that increasing the number of degrees of freedom (in this case, allowing for more hyperons) always yield softer equations of state and more compact stars.

Moreover, the purpose of this paper is not only to have another model for the structure of neutron stars with hyperons, but also to prepare the ground for the calculation of neutrino-nucleon scattering within the same framework [16], for which a knowledge of the interaction in the spin $S = 1$ channel is needed. Since neither the model of Balberg and Gal [2] nor that of Banik and Bandyopadhyay [24] provide us information on polarized systems, they do not allow to study the ferromagnetic criterion when the Σ^- are taken into account.

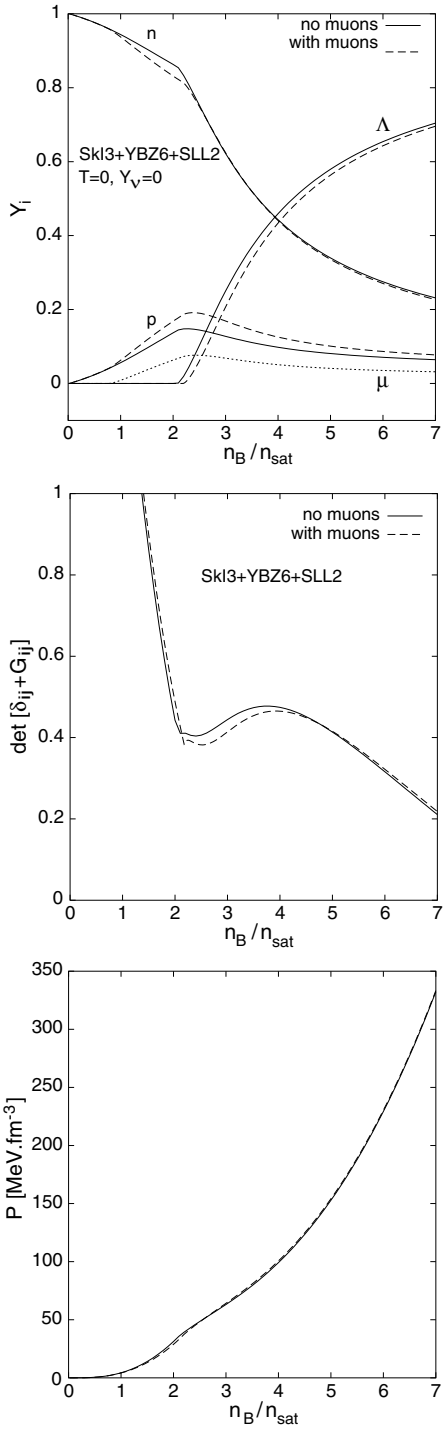

Fig. 8. Effects of muons on the chemical composition, ferromagnetic criterion and equation of state.

As mentioned in the introduction, only the Λ-hyperons are considered in the models presented in the previous sections because this study is restricted to potentials available in the literature, thus offering some guarantee that they correctly reproduce the properties of nuclear matter as well as the experimental data on nuclei and hypernuclei. In order to ascertain the important point whether $np\Lambda\Sigma$

Table 8. Parameters of Dabrowski's ΣN interaction (quoted in MeV) and threshold densities (in units of the saturation density) for the formation of Σ and Λ hyperons in matter in β equilibrium. The values are quoted with/(without) muons taken into account.

					(SkI3 + YBZ6 + SLL2)		(SLy10 + LYI + SLL2)	
	$\mathcal{U}_0$	$\mathcal{U}_\tau$	$\mathcal{U}_\sigma$	$\mathcal{U}_{\sigma\tau}$	$n_{\rm thr}^{\Sigma^-}$	$n_{\rm thr}^{\Lambda}$	$n_{\rm thr}^{\Sigma^-}$	$n_{\rm thr}^{\Lambda}$
model D	−13.1	55.1	66.8	63.9	1.57 (1.50)	5.64 (5.85)	2.50 (2.47)	2.92 (2.94)
model F	23.5	20.4	72.3	95.6	2.03 (1.89)	2.52 (2.57)	4.92 (4.86)	2.73 (2.73)

matter is stable against spin fluctuations, let us nevertheless deviate for a moment from this line of conduct.

There is actually some data on the Σ^- available in the papers by Dabrowski [21]. This author calculated the single-particle potential $\mathcal{U}(k_\Sigma, n_B)$ felt by a Σ impurity in nuclear matter:

$$\mathcal{U}_{\Sigma^-\uparrow/\downarrow}(k_\Sigma, n_B) = \mathcal{U}_0 - \frac{1}{2}\alpha_\tau \mathcal{U}_\tau + \frac{1}{4}\alpha_\sigma \mathcal{U}_\sigma \mp \frac{1}{2}\alpha_{\sigma\tau}\mathcal{U}_{\sigma\tau} \quad (14)$$

with
$$\alpha_\tau = \frac{\rho_p - \rho_n}{\rho_p + \rho_n}\,,$$
$$\alpha_\sigma = \frac{\rho_{p\uparrow} + \rho_{n\uparrow} - \rho_{p\downarrow} - \rho_{n\downarrow}}{\rho_p + \rho_n}\,,$$
$$\alpha_{\sigma\tau} = \frac{\rho_{p\uparrow} - \rho_{p\downarrow} - \rho_{n\uparrow} + \rho_{n\downarrow}}{\rho_p + \rho_n}$$

Dabrowski quotes numerical values for the $\mathcal{U}_i$ taken at the point $k_\Sigma = 0$, $n_B = n_{\rm sat}$ (which are reproduced in table 8, all values being given in MeV) for several variants of the Nijmegen potential. "Model D" and "model F", while not the most modern Nijmegen potentials available, are representative of an attractive (respectively, repulsive) $N\Sigma^-$ interaction potential in nuclear matter. Model F is favoured by Dabrowski for the description of hypernuclei as well as of the data collected at BNL on the (K^-, π^+) reaction.

In order to address the question of the influence of the Σ^- in the $S = 1$ channel, we may try to extrapolate this data as follows: From $\mathcal{U}(k_\Sigma, n_B)$ we may extract the chemical potential $\mu_\Sigma = (\hbar^2/2m_\Sigma^*)k_{F\Sigma}^2 + \mathcal{U}(0, \rho_p + \rho_n)$. We will take the effective mass of the Σ^- constant and equal to the free mass, an assumption supported by the Brueckner calculations of Vidaña *et al.* [27] or Baldo *et al.* [28]. We will assume the single-particle potential to depend linearly on the nucleonic density, which is equivalent to neglecting t_3-like terms representative of many-body effects (see, *e.g.*, appendix A, eqs. (A.7), (A.8)). Note also that only the $N\Sigma$ contribution to the chemical potential is thus taken into account, while $\Lambda\Sigma$ or $\Sigma\Sigma$ contributions are ignored. Finally, the Landau parameters $g_{n\Sigma^-}$ and $g_{p\Sigma^-}$ can be identified with the spin components of the single-particle potential:

$$g_{n\Sigma^-} = \frac{1}{4(\rho_n + \rho_p)}\left[\mathcal{U}_\sigma + 2\mathcal{U}_{\sigma\tau}\right]\,,$$
$$g_{p\Sigma^-} = \frac{1}{4(\rho_n + \rho_p)}\left[\mathcal{U}_\sigma - 2\mathcal{U}_{\sigma\tau}\right] \quad (15)$$

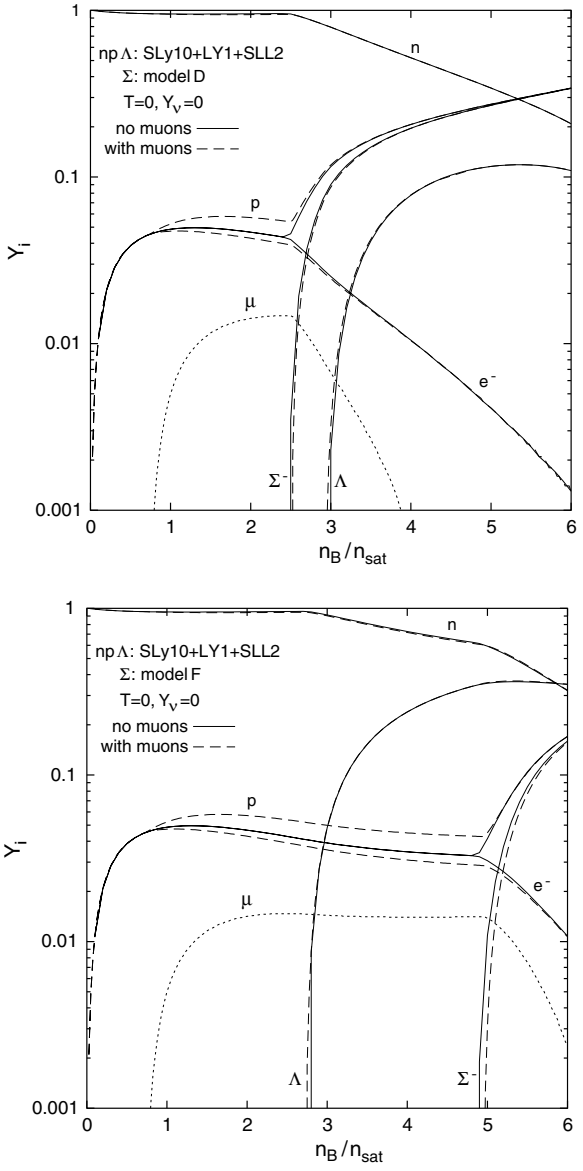

Fig. 9. Chemical composition of $np\Lambda\Sigma^- e^- \mu^-$ matter in β equilibrium. The interaction is chosen to be (SLy10 + LYI + SLL2) for the $np\Lambda$ subsystem. The $N\Sigma$ interaction is described by Nijmegen models D (top panel) or F (bottom panel).

The chemical equilibrium is obtained by applying the same conditions as before on the chemical potential (see sect. 3), supplemented by the condition for β equilibrium on the Σ^- fraction $\mu_{\Sigma^-} = \mu_\Lambda + \mu_n - \mu_p$. The particle fractions obtained in this way are shown in fig. 9.

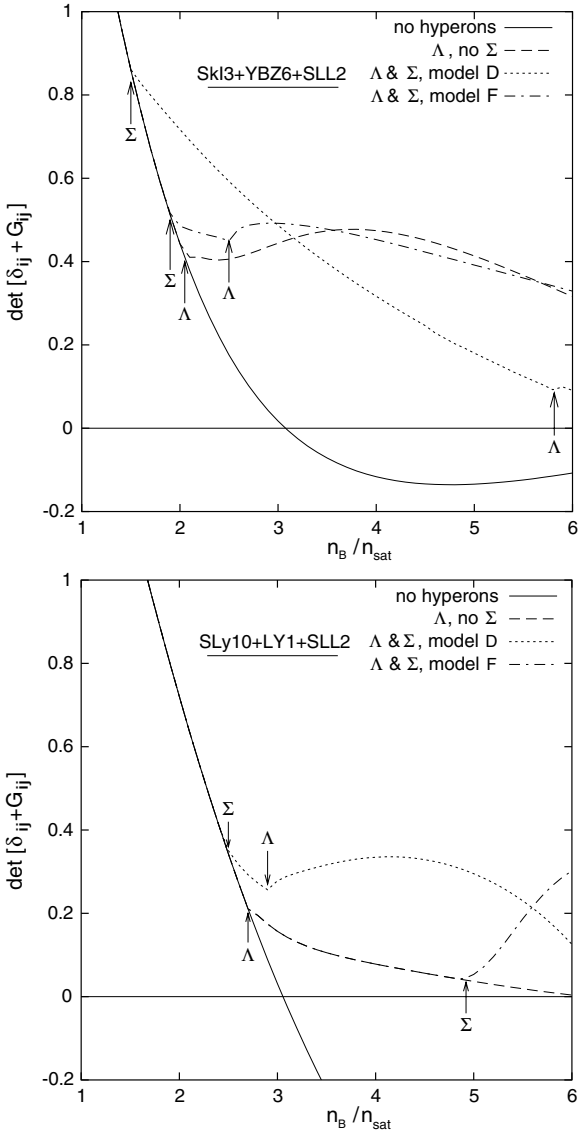

Fig. 10. Ferromagnetic criterion in $npA\Sigma^-e^-\mu^-$ matter in β equilibrium.

The interaction is chosen to be (SkI3 + YBZ6 + SLL2) or (SLy10 + LYI + SLL2) for the npA subsystem. When (SLy10 + LYI + SLL2) is used, the Σ^- appear at lower density than the A for model D, while they appear after the A for model F. When (SkI3 + YBZ6 + SLL2) is used, the Σ^- appear earlier than the A in both cases. Let us notice that the characterization of models D and F as, respectively, "attractive" and "repulsive" loses some of its significance, since we are dealing with matter with a strong n:p asymmetry, and the attractive $\mathcal{U}_0$ interaction of the D model is compensated by a strongly repulsive $\mathcal{U}_\tau$ in the isospin channel. The threshold densities are given in table 8. Values with (without) parentheses represent threshold in matter without (with) muons. Again we can see that the presence of muons does not appreciably affect the results. Some threshold densities obtained in this way are somewhat low (see, *e.g.*, $n_{\rm thr}^{\Sigma}$ with the parametrization (SkI3 + YBZ6 + SLL2) + (model D)), reflecting the crudeness of the approximations performed here.

The ferromagnetic criterion is now given by the determinant of the 4×4 matrix (see eq. (13))

$$\mathrm{Det}[\delta_{ij} + G_{ij}] = \mathrm{Det}\begin{pmatrix} (1+G_0^{nn}) & G_0^{np} & G_0^{n\Lambda} & G_0^{n\Sigma^-} \\ G_0^{pn} & (1+G_0^{pp}) & G_0^{p\Lambda} & G_0^{p\Sigma^-} \\ G_0^{\Lambda n} & G_0^{\Lambda p} & (1+G_0^{\Lambda\Lambda}) & G_0^{\Lambda\Sigma^-} \\ G_0^{n\Sigma^-} & G_0^{p\Sigma^-} & G_0^{\Lambda\Sigma^-} & (1+G_0^{\Sigma^-\Sigma^-}) \end{pmatrix}.$$

From this model it is found (see fig. 10) that the Σ-hyperons do not spoil the behavior of the ferromagnetic criterion observed in sect. 4. A more detailed study involving a better knowledge of the interaction of the Σ with all baryons, and especially its dependence on the density and chemical composition of the matter, is however desirable before we can draw definite conclusions on that subject.

Let us, to conclude this section, stress again some of the weaknesses of the procedure used here to model the ΣN interaction:

- One obviously questionable step is the drastic assumption performed as to the density dependence of the various components of the potential, in particular the lack of information on the density dependence in the $S = 1$ channel;
- Since Dabrowski is interested in hypernuclei, he does not provide information on the ΣA and $\Sigma\Sigma$ interactions. They were here set equal to zero, in spite of the known importance of the N-Σ-A coupling in Brueckner calculations, and even though we have seen how sensitive the results were to the AA interaction;
- It is known that the various Nijmegen potentials display a large variability in their description of the spin-spin interaction, and little is known about the strength and even sign of this component.

7 Finite-temperature effects, neutrino trapping

According to proto-neutron star formation and cooling calculations (see, *e.g.*, [30]), temperatures of the order of 30 to 50 MeV can be reached in the late phases of the supernova collapse. We therefore investigate here the range $T \in [0\text{–}50]$ MeV.

The thermodynamical quantities are now to be written in terms of Fermi integrals. The expressions which are given in the appendix at $T = 0$ are easily generalized: The densities ρ_i and the quantities τ_i related to the kinetic energy should be replaced in the expressions for the baryonic contributions to the energy density and the effective

masses by (in units $\hbar = c = k_B = 1$):

$$\rho_i = \frac{1}{2\pi^2}\,(2m_i^* T)^{3/2}\, I_{1/2}(\eta_i)\,,$$
$$\tau_i = \frac{1}{2\pi^2}\,(2m_i^* T)^{5/2}\, I_{3/2}(\eta_i)$$
$$\text{with} \qquad I_n = \int_0^\infty \frac{u^n \mathrm{d}u}{1+e^{u-\eta_i}}\,,$$

while the chemical potentials is related to the η_i by $\mu_i = \eta_i T + \mathcal{U}_i(\rho_i, \tau_i)$. The pressure is obtained from the derivative of the free energy:

$$\mathcal{F} = \mathcal{E} - T\mathcal{S}\,, \qquad \mathcal{E} = \sum_{A,B=N,\Lambda} \mathcal{E}_{AB} + \mathcal{E}_{\text{leptons}}\,,$$
$$P = \rho^2 \frac{\partial^2(\mathcal{F}/\rho)}{\partial \rho^2}$$

with the entropy

$$S = \sum_{i=n,p,\Lambda} S_i + S_{\text{leptons}}\,, \qquad S_i = \frac{5\tau_i}{6m_i^* T} - \rho_i\,\eta_i\,.$$

We used the GFD_D3 code published by Gong *et al.* [31] to calculate the Fermi integrals and keep as before the leptons fully relativistic, whereas the baryons are treated non-relativistically in consistency with the use of the Skyrme interaction.

The effect of temperature on the effective masses begins to be significant at $T \geq 30$ MeV; it tends to increase the neutron mass and decrease the proton effective mass, so that their difference is reduced. The presence of trapped neutrinos, which tends to render the matter less asymmetric, also reduces the proton-neutron mass difference. In a warm protoneutron star, both effects are present and cumulate, the main contribution coming from $Y_\nu \neq 0$. The hyperon mass, on the other hand, is not significantly modified by temperature or neutrino trapping.

The chemical composition is plotted in fig. 11, without neutrino trapping in the top panel and with neutrino trapping in the bottom panel, for four values of the temperature, $T = 0$, 10, 20 and 50 MeV. We used in this section the parametrization SkI3 + YBZ6 + SLL2.

Let us first discuss the neutrino-free case. It can be seen in fig. 11 (top) that finite-temperature effects are more important at moderate densities, $n_B < 3n_{\text{sat}}$. Until $T = 1$ MeV the results are undistinguishable from the $T = 0$ case. When T is increased from 1 to 50 MeV, the matter is more symmetric (*i.e* the proton fraction increases). There is *stricto sensu* no threshold for Λ-hyperon production anymore, rather there always exist a vanishingly small number of Λ's for any value of the baryonic density below the $T = 0$ threshold. Nevertheless, at the temperatures considered here, it is still possible to define a threshold density for practical purposes, which then moves to lower values as the temperature increases.

The equation of state is somewhat stiffer at finite T, but this hardly affects the structure of the star until $T = 20$ MeV. This result concerns the case when no neutrinos are present in the matter. It is known, however, that

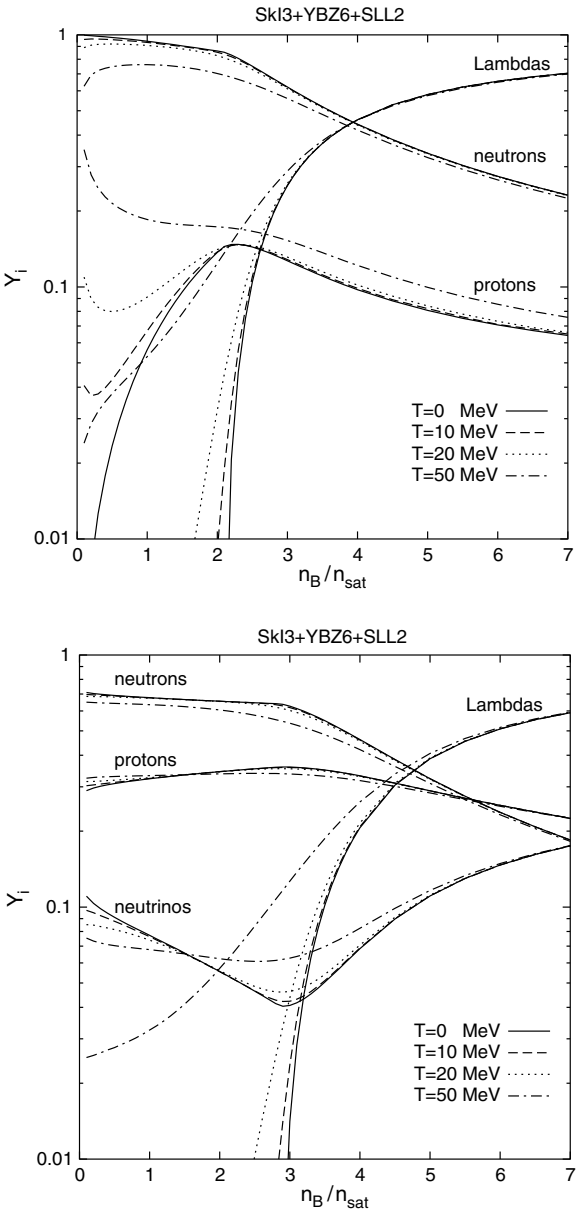

Fig. 11. Composition of neutron star matter in β equilibrium at finite temperature, calculated with the parametrization SkI3 + YBZ6 + SLL2 (top) without neutrino trapping, (bottom) with neutrino trapping, $Y_L = 0.4$.

high temperature shortens drastically the mean free path of the neutrinos, so that a large amount of ν are trapped. A typical value resulting from supernova collapse calculations is that the lepton fraction is of the order of $Y_L \simeq 0.4$. Figure 11 (bottom) was drawn assuming this value for Y_L.

As expected, the matter is more symmetric when neutrinos are trapped and the threshold for hyperon production is shifted to higher density. For example, with the SkI3 + YBZ6 + SLL2 parametrization and at $T = 0$ we have ($n_{\text{thr}} = 2.08$, $Y_p^{\text{thr}} = 0.14$) for $Y_\nu = 0$ and ($n_{\text{thr}} = 2.84$, $Y_p^{\text{thr}} = 0.36$) for $Y_L = 0.4$. For a given lepton fraction Y_L, varying the temperature has even less impact on the composition of neutrino-trapped matter than

Table 9. Influence of temperature on neutron star properties.

SkI3 + YBZ6 + SLL2	$n_{\rm ferro}$	$n_{c_s^2=1}$	$n_c(1.4\ M_\odot)$	$R(1.4\ M_\odot)$	$n_{\rm max}$	$M_{\rm max}$	$R(M_{\rm max})$
$T = 0$, $Y_\nu = 0$	9.19	13.08	2.39	13.19	6.79	1.64	11.02
$T = 30$ MeV, $Y_L = 0.4$	11.37	12.02	2.66	15.11	6.38	1.88	12.08

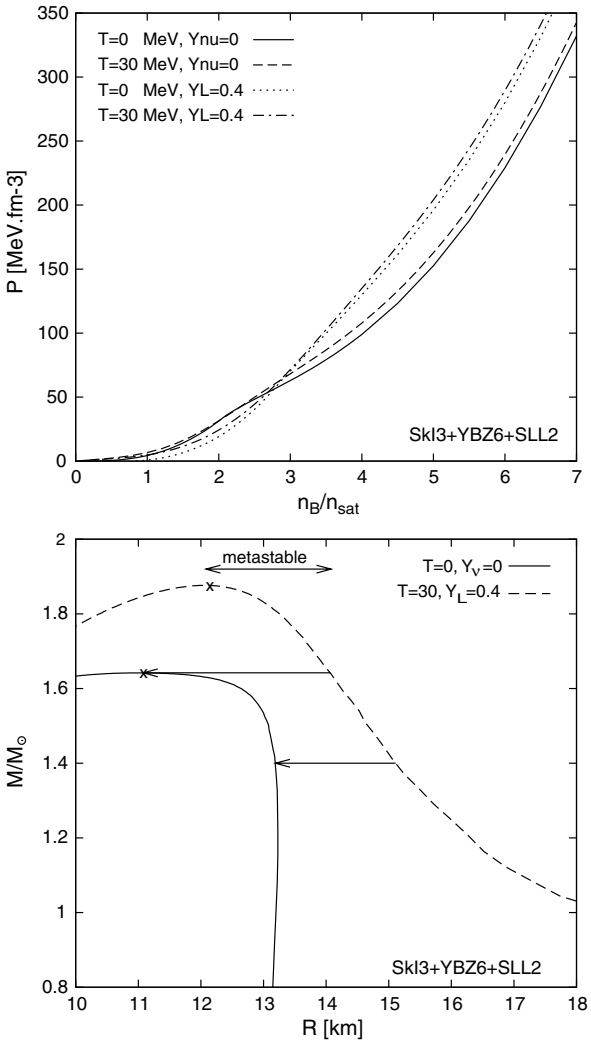

Fig. 12. Effect of neutrino trapping and finite temperature on (top) the equation of state; (bottom) the structure of the neutron star.

in neutrino-free matter. Figure 12 (top) shows that the neutrino-trapped matter with hyperons is stiffer than its neutrino-free counterpart, a known result which leads to interesting consequences regarding a possible category of metastable stars which would collapse to a black hole as they cool when the deleptonization phase is completed (see, *e.g.*, [32]). Figure 12 (bottom) illustrates this feature for the parameter set SkI3 + YBZ6 + SLL2: A newly formed protoneutron star with $T = 30$ MeV and $Y_L = 0.4$ is metastable if its mass lies in the range $M \in [1.64\text{–}1.88]\ M_\odot$ (and the radius in the range $R \in [12.08\text{–}14.07]$ km). For a lower mass, the star contracts as it looses its neutrinos and cools and its hyperonic content increases (see table 9).

As a conclusion to this subsection, our results concerning the effects of temperature and neutrino trapping are in full agreement with those obtained with other models of the baryonic interaction. The influence of the temperature on the equation of state and chemical equilibrium comes mostly indirectly through the buildup of an important fraction of trapped neutrinos.

8 Conclusion

The aim of this work was threefold:

- Use the most recent Skyrme parametrizations with hyperons existing on the market which are adjusted to reproduce the data on nuclei and hypernuclei and test them on neutron stars;
- Study the influence of the hyperons on the ferromagnetic transition;
- Inquire whether the hyperons are likely to affect the tail of the neutrino burst in supernova explosions and prepare the background for the calculation of the neutrino mean free path in protoneutron stars.

While the model considered in this work is still very schematic, it has led to several interesting results.

The first result is that the presence of hyperons generally delays the onset of the ferromagnetic instability, and in many cases they are even able to remove it completely.

Another advantage is that, by softening the equation of state, the hyperons remove the causality flaw and keep $c_s^2 < 1$ even up to very large densities.

It is rather encouraging that NN and $N\Lambda$ interactions from different authors and apparently very dissimilar parameter sets (compare, *e.g.*, SV to SkI3 or SKSH1 to LY-I in tables 1, 2!), once a series of reasonable requirements are fulfilled, yield very similar results qualitatively and even quantitatively. The major incognita is the $\Lambda\Lambda$ interaction which was very poorly known at the time the interactions used in this work were designed.

After studying 44 NN forces in combination with 13 parametrizations of the $N\Lambda$ force and 4 options for the $\Lambda\Lambda$ forces, all taken from the literature and known to reproduce correctly the properties of nuclei and hypernuclei, four combinations of $NN + N\Lambda + \Lambda\Lambda$ parameter sets were selected: (SkI3 + YBZ6 + no $\Lambda\Lambda$), (SkI3 + YBZ6 + SLL2), (SV + YBZ6 + SLL2) and (SLy10 + LYI + SLL2). Replacing SkI3 by SkI5 or LYI by LYIV in the above sets would only give slightly different results. These sets fulfill all of the following conditions:

i) The NN force belongs to the subset selected by Rikovska Stone *et al.* The effective masses behave

smoothly in all the relevant density and temperature range, pure neutron matter is always stable, the asymmetry energy does not decrease so much with density that protons would disappear from the system, neutron stars formed from *npe* matter in β equilibrium can reach a mass at least equal to 1.4 $M_\odot$.

ii) The $N\Lambda$ force belongs to the set preferred by Lanskoy *et al.* as best reproducing the properties of hypernuclei. The threshold for hyperon formation should lay between 1.7 and 4 times saturation.

iii) The neutron star formed of softer $np\Lambda e$ matter in β equilibrium should still reach a mass at least equal to 1.4 $M_\odot$.

iv) No ferromagnetic transition should be present As explained in the main text, this is, for a Skyrme parametrization, a strong requirement.

The second result of this work is that the selected sets are also found to reproduce all features observed in other models such as non-relativistic Brueckner-Hartree-Fock or relativistic mean-field calculations, not only qualitatively but also quantitatively. The threshold for hyperon formation is in fact restricted to the narrower range [2–2.5] $n_{\rm sat}$. The softening of the equation of state brings the maximum mass of the star from 2–2.5 $M_\odot$ for a *npe* star down to 1.4–1.6 $M_\odot$ for a *npYe* star. This has even led to some speculation (see, *e.g.*, [27]) whether the clustering of known pulsar masses around the value 1.4 $M_\odot$ would be due to this feature of the equation of state rather than to the circumstances of their formation in a supernova. The metastability of hot stars with trapped neutrinos when hyperons are present, as discussed, *e.g.*, in [32], is also recovered.

The selected sets are also applied in a companion paper [16] to the calculation of the scattering rate of neutrinos in baryonic matter, for a finite temperature and non-vanishing number of trapped neutrinos. The possibility to access the properties of polarized matter was a further motivation to this work: It was necessary to be able to calculate the Landau parameters in the spin $S = 1$ channel, since the axial channel is dominant for neutrino scattering.

As a protoneutron star is formed in a supernova explosion, the high amount of neutrinos trapped in its interior by high temperature and density gradually diffuse out in the first 50 seconds as the star cools. Hyperons begin to appear in the course of this deleptonization process and could affect the tail of the neutrino signal. Modern detectors would now be able to detect this effect. The idea was explored by Reddy *et al.* [33] in the mean-field approximation. The calculation is performed in the random phase approximation in [16]. The parameter sets selected in the present work predict a non-negligible hyperon content for $t \geq 20$ s after the collapse (see figs. 2 and 3 of [16]).

Let us examine again the main shortcomings of the present model and the way it could be improved in future work.

i) The Skyrme interaction has long been known for displaying a series of problems at high density: behavior of asymmetry energy, onset of ferromagnetism, causality, ... While we were able to avoid these problems by carefully passing the existing parametrizations through the crib of these various constraints, we cannot avoid the feeling that we are pushing the Skyrme model much beyond its capacity. More refined models do not have these problems; for example, the non-relativistic Brueckner-Hartree-Fock calculations do not show a ferromagnetic transition. A possible answer to this point would be to develop a parametrization of Brueckner-Hartree-Fock calculations in terms of an energy density functional for polarized matter with a non-vanishing hyperonic content. Some steps have already been performed in this direction by Vidaña *et al.* These authors studied the polarized neutron-proton matter system [12] and concluded to the absence of a ferromagnetic transition. They also obtained the equation of state of unpolarized *npY* matter in β equilibrium and applied it to the calculation of neutron star mass radius relation [27] and parametrized the neutron-proton-Lambda system [34] for applications to hypernuclei. The parametrization of Brueckner-Hartree-Fock results with modern Nijmegen potentials for the full polarized $np\Lambda\Sigma$ is currently under way [35].

ii) We have seen that the effect of the $\Lambda\Lambda$ force at high density is very important, whereas the description of the hyperon-hyperon interaction in phenomenological formalisms is still very poor. Brueckner-Hartree-Fock calculations offer a coherent framework to calculate the hyperon-hyperon interaction in medium starting from bare potentials such as the Nijmegen one known from scattering data of free particles, and then cross-checking the results with the data on double hypernuclei. This has actually been performed with the Nijmegen NSC97e model, *e.g.*, in [36].

iii) Relativistic effects can be expected to play an important role at high density. Many of the problems encountered in the Skyrme parametrization mentioned above in this paragraph (behavior of asymmetry energy, onset of ferromagnetism and causality) are not present in the relativistic formulation. Relativistic mean-field models with hyperons (see, *e.g.*, [37]) are so well under control that they have made their way into textbooks [38]. The parametrizations of the present work obviously do not pretend to compete with this line of work at the mean-field level; rather, they were developed in view of their application at the RPA level where they give rise to simpler Dyson equations than in the relativistic formulation. The relativistic extension at RPA level to hyperons would be completely straightforward but somewhat unwieldy.

While it could be argued that the physical foundations of the Skyrme model are disputable when applied in the context of neutron stars, the parametrizations presented in this paper should rather be considered as reliable phenomenological models for run-of-the-mill calculations. Once the orders of magnitude of physical effects are ascertained with this simple model, they can be refined by applying more complicated Brueckner-Hartree-Fock or/and relativistic models.

This work was supported by the Spanish-European (FICYT/FEDER) grant number PB02-076. Part of it was realized during a stay at the Departament d'Estructura i Constituents de la Materia of Barcelona University. Several discussions with A. Polls are gratefully acknowlegded.

Appendix A.

Besides the the usual parameterization of the nucleon-nucleon interaction

$$\begin{aligned}V_{NN}(r_1-r_2) &= t_0\,(1+x_0P_\sigma)\delta(r_1-r_2)\\ &+\frac{1}{2}t_1\,(1+x_1P_\sigma)\left[k'^2\;\delta(r_1-r_2)+\delta(r_1-r_2)\;k^2\right]\\ &+t_2\,(1+x_2P_\sigma)k'\,\delta(r_1-r_2)\,k\\ &+\frac{1}{6}t_3\,(1+x_3P_\sigma)\,\rho_N^\alpha\left(\frac{r_1+r_2}{2}\right)\delta(r_1-r_2),\end{aligned}\tag{A.1}$$

we use the following Lambda-nucleon and Lambda-Lambda potentials [4,5]:

$$\begin{aligned}V_{N\Lambda}(r_N-r_\Lambda) &= u_0\,(1+y_0P_\sigma)\delta(r_N-r_\Lambda)\\ &+\frac{1}{2}u_1\;\left[k'^2\;\delta(r_N-r_\Lambda)+\delta(r_N-r_\Lambda)\;k^2\right]\\ &+u_2\,k'\,\delta(r_N-r_\Lambda)\,k+\frac{3}{8}u_3\,(1+y_3P_\sigma)\\ &\times\rho_N^\beta\left(\frac{r_N+r_\Lambda}{2}\right)\delta(r_N-r_\Lambda),\end{aligned}\tag{A.2}$$

$$\begin{aligned}V_{\Lambda\Lambda}(r_1-r_2) &= \lambda_0\delta(r_1-r_2)\\ &+\frac{1}{2}\lambda_1\left[k'^2\;\delta(r_1-r_2)+\delta(r_1-r_2)\;k^2\right]\\ &+\lambda_2\,k'\,\delta(r_1-r_2)\,k+\lambda_3\,\rho_\Lambda\rho_N^\gamma\end{aligned}\tag{A.3}$$

(we haved dropped in these expressions the spin-orbit terms which are not used in this paper). We obtain the energy density in homogeneous matter in the usual way. In spin saturated $npΛ$ matter, the functional reads:

$$\begin{aligned}\mathcal{E} &= \langle\psi\,|\,H\,|\,\psi\rangle = \mathcal{E}_{NN}+\mathcal{E}_{N\Lambda}+\mathcal{E}_{\Lambda\Lambda}\,,\\ \mathcal{E}_{NN} &= \frac{\hbar^2}{2m_N}\tau_N\\ &+\frac{t_0}{2}\left[\left(1+\frac{x_0}{2}\right)\rho_N^2-\left(\frac{1}{2}+x_0\right)(\rho_n^2+\rho_p^2)\right]\\ &+\frac{t_3}{12}\rho_N^\alpha\left[\left(1+\frac{x_3}{2}\right)\rho_N^2-\left(\frac{1}{2}+x_3\right)(\rho_n^2+\rho_p^2)\right]\\ &+\frac{1}{8}\left[t_1(2+x_1)+t_2(2+x_2)\right]\rho_N\tau_N\\ &-\frac{1}{8}\left[t_1(2x_1+1)-t_2(2x_2+1)\right](\rho_n\tau_n+\rho_p\tau_p)\,,\end{aligned}\tag{A.4}$$

$$\begin{aligned}\mathcal{E}_{N\Lambda} &= u_0\left(1+\frac{y_0}{2}\right)\rho_N\rho_\Lambda+\frac{3}{8}u_3\,\rho_N^{\beta+1}\rho_\Lambda\left(1+\frac{y_3}{2}\right)\\ &+\frac{1}{8}\left[u_1(2+y_1)+u_2(2+y_2)\right](\rho_N\tau_\Lambda+\rho_\Lambda\tau_N)\,,\end{aligned}\tag{A.5}$$

$$\mathcal{E}_{\Lambda\Lambda} = \frac{\hbar^2}{2m_\Lambda}\tau_\Lambda+\frac{\lambda_0}{4}\rho_\Lambda^2+\frac{1}{8}(\lambda_1+3\lambda_2)\,\rho_\Lambda\tau_\Lambda+\frac{\lambda_3}{4}\,\rho_\Lambda^2\rho_N^\gamma\tag{A.6}$$

with $\rho_N=\rho_n+\rho_p$, $\tau_N=\tau_n+\tau_p$. At $T=0$ we have $\tau_i=(3/5)\,\rho_i k_{Fi}^2$ and $\rho_i=k_{Fi}^3/(3\pi^2)$. At $T\neq 0$ these expressions should be replaced by Fermi integrals, see sect. 7. At $T=0$ we obtain the chemical potentials

$$\begin{aligned}\mu_n &= \frac{\partial\mathcal{E}}{\partial\rho_n}=\frac{\hbar^2}{2m_n^*}k_{Fn}^2+\mathcal{U}_n(\rho_i,\tau_i)\,,\\ \mathcal{U}_n(\rho_i,\tau_i) &= \frac{t_0}{2}\left[\rho_n(1-x_0)+\rho_p(2+x_0)\right]\\ &+\frac{t_3}{24}\rho_N^{\alpha-1}\Big[\rho_n^2\left\{(2+\alpha)(1-x_3)\right\}+\rho_p^2\{2\,(2+x_3)\\ &+\alpha(1-x_3)\}+2\rho_n\rho_p\left\{3+\alpha(2+x_3)\right\}\Big]\\ &+\frac{1}{8}\left[t_1(1-x_1)+3t_2(1+x_2)\right]\tau_n\\ &+\frac{1}{8}\left[t_1(2+x_1)+t_2(2+x_2)\right]\tau_p+\frac{\lambda_3}{4}\gamma\rho_\Lambda^2\rho_N^{\gamma-1}\\ &+u_0\left(1+\frac{y_0}{2}\right)\rho_\Lambda+\frac{3}{8}u_3(\beta+1)\left(1+\frac{y_3}{2}\right)\rho_N^\beta\rho_\Lambda\\ &+\frac{1}{8}\left[u_1(2+y_1)+u_2(2+y_2)\right]\tau_\Lambda\end{aligned}\tag{A.7}$$

(the chemical potential for the proton μ_p can be obtained from μ_n by interchanging the indices n and p) and

$$\begin{aligned}\mu_\Lambda &= \frac{\partial\mathcal{E}}{\partial\rho_\Lambda}=\frac{\hbar^2}{2m_\Lambda^*}k_{F\Lambda}^2++\mathcal{U}_\Lambda(\rho_i,\tau_i)\,,\\ \mathcal{U}_\Lambda(\rho_i,\tau_i) &= \frac{\lambda_0}{2}\rho_\Lambda+\frac{\lambda_3}{2}\rho_N^\gamma\rho_\Lambda+\frac{1}{8}(\lambda_1+3\lambda_2)\tau_\Lambda\\ &+u_0\left(1+\frac{y_0}{2}\right)\rho_N+\frac{3}{8}u_3\left(1+\frac{y_3}{2}\right)\rho_N^{\beta+1}\\ &+\frac{1}{8}[u_1(2+y_1)+u_2(2+y_2)]\tau_N\,.\end{aligned}\tag{A.8}$$

The effective masses are given by

$$\begin{aligned}\frac{\hbar^2}{2m_n^*} &= \frac{\hbar^2}{2m_N}+\frac{1}{8}\left[t_1(2+x_1)+t_2(2+x_2)\right]\rho_N\\ &-\frac{1}{8}\left[t_1(2x_1+1)-t_2(2x_2+1)\right]\rho_n\\ &+\frac{1}{8}\left[u_1(2+y_1)+u_2(2+y_2)\right]\rho_\Lambda\end{aligned}\tag{A.9}$$

(the effective mass of the proton follows from replacing ρ_n by ρ_p in this expression) and

$$\begin{aligned}\frac{\hbar^2}{2m_\Lambda^*} &= \frac{\hbar^2}{2m_\Lambda}+\frac{1}{8}\left[\lambda_1+3\lambda_2\right]\rho_\Lambda\\ &+\frac{1}{8}\left[u_1(2+y_1)+u_2(2+y_2)\right]\rho_N\,.\end{aligned}\tag{A.10}$$

For deriving the Landau parameters we will also need the polarized energy functional $\mathcal{E}(\rho_{n\uparrow},\rho_{n\downarrow},\rho_{p\uparrow},\rho_{p\downarrow},\rho_{\Lambda\uparrow},\rho_{\Lambda\downarrow})$. We do not reproduce this somewhat

lengthy expression here, but note that it coincides for np matter with the functional given by Bender *et al.* [39].

The Landau parameters in the monopolar approximation $\ell = 0$ can be calculated in the following way. We first take the derivative of the single-particle energies (or, equivalently, the second functional derivative of the energy density with respect to occupation numbers $\rho_i(k)$):

$$f_{\tau_1\sigma_1\tau_2\sigma_2} := \left(\frac{\mathrm{d}U_{\tau_1\sigma_1}(k)}{\mathrm{d}\rho_{\tau_2\sigma_2}}\right)_{|k=k_{F\tau_1\sigma_1}} ; \tag{A.11}$$

$$f_{\tau_1\sigma_1\tau_2\sigma_2} = f_{\tau_2\sigma_2\tau_1\sigma_1} , \qquad \tau \in \{n, p, \Lambda\} , \ \sigma \in \{\uparrow, \downarrow\} .$$

In the Skyrme model the single-particle energies $U_{\tau\sigma}(k)$ are quadratic in the momentum k:

$$U_{\tau\sigma}(k) := U_{\tau\sigma} + \frac{\hbar^2}{m^*_{\tau\sigma}}k^2 \tag{A.12}$$

and related to the chemical potentials in polarized matter:

$$\mu_{\tau\sigma} := \left(\frac{\mathrm{d}\mathcal{E}}{\mathrm{d}\rho_{\tau\sigma}}\right)_{|\rho(\tau'\sigma'\neq\tau\sigma)=cst} =$$

$$U_{\tau\sigma} + \frac{\hbar^2}{m^*_{\tau\sigma}}k^2_{F\tau\sigma} = U_{\tau\sigma}(k_{F\tau\sigma}) \tag{A.13}$$

with $\rho_{\tau\sigma} = k^3_{F\tau\sigma}/(6\pi^2)$ at $T = 0$.

The Landau parameters in the spin $S = 0$ channel are obtained from

$$f_{\tau_1\tau_2} := \frac{1}{4}\left[f_{\tau_1\uparrow\tau_2\uparrow} + f_{\tau_1\downarrow\tau_2\downarrow} + f_{\tau_1\uparrow\tau_2\downarrow} + f_{\tau_1\downarrow\tau_2\uparrow}\right]_{|\text{unpolarized}} \tag{A.14}$$

and in the spin $S = 1$ channel from

$$g_{\tau_1\tau_2} := \frac{1}{4}\left[f_{\tau_1\uparrow\tau_2\uparrow} + f_{\tau_1\downarrow\tau_2\downarrow} - f_{\tau_1\uparrow\tau_2\downarrow} - f_{\tau_1\downarrow\tau_2\uparrow}\right]_{|\text{unpolarized}} . \tag{A.15}$$

The $f_{\tau_1\tau_2}$ are related to usual thermodynamical quantities, for example the compressibility and the asymmetry energy

$$K = \frac{3k_F^2}{m^*_N}(1 + F_0) , \qquad a_{\text{asym}} = \frac{k_F^2}{6m^*_N}(1 + F'_0) \tag{A.16}$$

$$\text{with} \quad k_F = k_{Fn} = k_{Fp} , \qquad f_{nn} = f_{pp} ,$$

$$f_0 = \frac{f_{pp} + f_{np}}{2} , \ f'_0 = \frac{f_{pp} - f_{np}}{2} ,$$

$$F_0 = N_0 \ f_0 , \quad F'_0 = N_0 \ f'_0 , \quad N_0 = \frac{2m^*_N k_F}{\pi^2}$$

in symmetric nuclear matter.

The $g_{\tau_1\tau_2}$ are related to the magnetic susceptibilities and are used to form the ferromagnetic criterion (eqs. (11)-(13))

Their explicit expressions are

In the spin $S = 0$ channel:

$$\begin{aligned} f_{nn} = {} & \frac{1}{2}t_0(1 - x_0) + \frac{1}{12}t_3\rho_N^\alpha(1 - x_3) + \frac{1}{3}\alpha t_3\rho_N^{\alpha-1} \\ & \times \left[\left(1 + \frac{x_3}{2}\right)\rho_N - \left(\frac{1}{2} + x_3\right)\rho_n\right] + \frac{1}{12}\alpha(\alpha - 1) \\ & \times t_3\rho_N^{\alpha-2}\left[\left(1 + \frac{x_3}{2}\right)\rho_N^2 - \left(\frac{1}{2} + x_3\right)(\rho_n^2 + \rho_p^2)\right] \\ & + \frac{1}{4}\left[t_1(1 - x_1) + 3t_2(1 + x_2)\right]k^2_{Fn} \\ & + \frac{3}{8}u_3\left(1 + \frac{y_3}{2}\right)\beta(\beta + 1)\rho_N^{\beta-1}\rho_\Lambda \\ & + \frac{1}{4}\lambda_3\gamma(\gamma - 1)\rho_N^{\gamma-2}\rho_\Lambda^2 , \end{aligned} \tag{A.17}$$

$$\begin{aligned} f_{np} = {} & t_0\left(1 + \frac{x_0}{2}\right) + \frac{1}{6}t_3\rho_N^\alpha\left(1 + \frac{x_3}{2}\right) \\ & + \frac{1}{4}\alpha t_3\rho_N^\alpha + \frac{1}{12}\alpha(\alpha - 1) \\ & \times t_3\rho_N^{\alpha-2}\left[\left(1 + \frac{x_3}{2}\right)\rho_N^2 - \left(\frac{1}{2} + x_3\right)(\rho_n^2 + \rho_p^2)\right] \\ & + \frac{1}{4}\left[t_1\left(1 + \frac{x_1}{2}\right) + t_2\left(1 + \frac{x_2}{2}\right)\right](k^2_{Fn} + k^2_{Fp}) \\ & + \frac{3}{8}u_3\left(1 + \frac{y_3}{2}\right)\beta(\beta + 1)\rho_N^{\beta-1}\rho_\Lambda \\ & + \frac{1}{4}\lambda_3\gamma(\gamma - 1)\rho_N^{\gamma-2}\rho_\Lambda^2 , \end{aligned} \tag{A.18}$$

$$\begin{aligned} f_{pp} = {} & \frac{1}{2}t_0(1 - x_0) + \frac{1}{12}t_3\rho_N^\alpha(1 - x_3) + \frac{1}{3}\alpha t_3\rho_N^{\alpha-1} \\ & \times \left[\left(1 + \frac{x_3}{2}\right)\rho_N - \left(\frac{1}{2} + x_3\right)\rho_p\right] + \frac{1}{12}\alpha(\alpha - 1) \\ & \times t_3\rho_N^{\alpha-2}\left[\left(1 + \frac{x_3}{2}\right)\rho_N^2 - \left(\frac{1}{2} + x_3\right)(\rho_n^2 + \rho_p^2)\right] \\ & + \frac{1}{4}\left[t_1(1 - x_1) + 3t_2(1 + x_2)\right]k^2_{Fp} \\ & + \frac{3}{8}u_3\left(1 + \frac{y_3}{2}\right)\beta(\beta + 1)\rho_N^{\beta-1}\rho_\Lambda \\ & + \frac{1}{4}\lambda_3\gamma(\gamma - 1)\rho_N^{\gamma-2}\rho_\Lambda^2 , \end{aligned} \tag{A.19}$$

$$\begin{aligned} f_{n\Lambda} = {} & \frac{1}{2}u_0(2 + y_0) + \frac{3}{16}u_3(2 + y_3)(1 + \beta)\rho_N^\beta \\ & + \frac{1}{8}\left[u_1(2 + y_1) + u_2(2 + y_2)\right](k^2_{F\Lambda} + k^2_{Fn}) \\ & + \frac{1}{2}\lambda_3\gamma\rho_N^{\gamma-1}\rho_\Lambda , \end{aligned} \tag{A.20}$$

$$\begin{aligned} f_{p\Lambda} = {} & \frac{1}{2}u_0(2 + y_0) + \frac{3}{16}u_3(2 + y_3)(1 + \beta)\rho_N^\beta \\ & + \frac{1}{8}\left[u_1(2 + y_1) + u_2(2 + y_2)\right](k^2_{F\Lambda} + k^2_{Fp}) \\ & + \frac{1}{2}\lambda_3\gamma\rho_N^{\gamma-1}\rho_\Lambda , \end{aligned} \tag{A.21}$$

$$f_{\Lambda\Lambda} = \frac{1}{2}\lambda_0 + \frac{1}{2}\lambda_3\rho_N^\gamma + \frac{1}{4}\left[\lambda_1 + 3\lambda_2\right]k^2_{F\Lambda} . \tag{A.22}$$

In the spin $S = 1$ channel:

$$g_{nn} = \frac{1}{2}t_0(x_0 - 1) + \frac{1}{12}t_3\rho_N^\alpha(x_3 - 1) + \frac{1}{4}\left[t_1(x_1 - 1) + t_2(1 + x_2)\right]k_{Fn}^2\,, \quad \text{(A.23)}$$

$$g_{np} = \frac{1}{2}t_0x_0 + \frac{1}{12}t_3x_3\rho_N^\alpha + \frac{1}{8}\left[t_1x_1 + t_2x_2\right](k_{Fn}^2 + k_{Fp}^2)\,, \quad \text{(A.24)}$$

$$g_{pp} = \frac{1}{2}t_0(x_0 - 1) + \frac{1}{12}t_3\rho_N^\alpha(x_3 - 1) + \frac{1}{4}\left[t_1(x_1 - 1) + t_2(1 + x_2)\right]k_{Fp}^2\,, \quad \text{(A.25)}$$

$$g_{n\Lambda} = \frac{1}{2}u_0y_0 + \frac{3}{16}u_3y_3\rho_N^\beta + \frac{1}{8}\left[u_1y_1 + u_2y_2\right](k_{F\Lambda}^2 + k_{Fn}^2)\,, \quad \text{(A.26)}$$

$$g_{p\Lambda} = \frac{1}{2}u_0y_0 + \frac{3}{16}u_3y_3\rho_N^\beta + \frac{1}{8}\left[u_1y_1 + u_2y_2\right](k_{F\Lambda}^2 + k_{Fp}^2)\,, \quad \text{(A.27)}$$

$$g_{\Lambda\Lambda} = -\frac{1}{2}\lambda_0 - \frac{1}{2}\lambda_3\rho_N^\gamma + \frac{1}{4}\left[-\lambda_1 + \lambda_2\right]k_{F\Lambda}^2\,. \quad \text{(A.28)}$$

In the limit where hyperons are absent, these expressions coincide with those of Hernández *et al.* [40].

References

1. E. Chabanat, P. Bonche, P. Haensel, J. Meyer, R. Schaeffer, Nucl. Phys. A **635**, 231 (1998).
2. A. Balberg, A. Gal, Nucl. Phys. A **625**, 435 (1997).
3. J. Rikovska Stone, J.C. Miller, R. Koncewicz, P.D. Stevenson, M.R. Strayer, Phys. Rev. C **68**, 034324 (2003).
4. D.E. Lanskoy, Y. Yamamoto, Phys. Rev. C **55**, 2330 (1997).
5. D.E. Lanskoy, Phys. Rev. C **58**, 3351 (1998).
6. F. Fernández, T. López Arias, C. Prieto, Z. Phys. **A**, 349 (1989).
7. A. Vidaurre, J. Navarro, J. Bernabeu, Astron. Astrophys. **135**, 361 (1984).
8. J. Margueron, J. Navarro, Nguyen Van Giai, Phys. Rev. C **66**, 014303 (2002).
9. J. Navarro, E.S. Hernandez, D. Vautherin, Phys. Rev. C **60**, 045801 (1999).
10. S. Reddy, M. Prakash, J.M. Lattimer, J.A. Pons, Phys. Rev. C **59**, 2888 (1999).
11. J. Margueron, PhD Thesis, Orsay University, France (2001).
12. I. Vidaña, I. Bombaci, Phys. Rev. C **66**, 045801 (2002); I. Vidaña, A. Polls, A. Ramos, Phys. Rev. C **65**, 035804 (2002).
13. W. Zuo, U. Lombardo, C.W. Shen, Phys. Rev. C **67**, 037301 (2003).
14. P. Bernardos, S. Marcos, R. Niembro, M.L. Quelle, Phys. Lett. B **356**, 175 (1995).
15. T. Maruyama, T. Tatsumi, Nucl. Phys. A **693**, 710 (2001).
16. L. Mornas, Eur. Phys. J. A **23**, 365 (2005).
17. P.G. Reinhard, H. Flocard, Nucl. Phys. A **584**, 467 (1995).
18. M. Beiner, H. Flocard, N. Van Giai, P. Quentin, Nucl. Phys. A **238**, 29 (1975).
19. Y. Yamamoto, H. Bandō, J. Žofka, Prog. Theor. Phys. **80**, 757 (1988).
20. Y. Yamamoto, H. Bandō, Prog. Theor. Phys. Suppl. **81**, 42 (1985); Y. Yamamoto, T. Motoba, H. Himeno, K. Ikeda, S. Nagata, Prog. Theor. Phys. Suppl. **117**, 361 (1994).
21. J. Dabrowski, Phys. Rev. C **60**, 025205 (1999); Acta Phys. Polon. B **35**, 971 (2004).
22. J. Mares, E. Friedman, A. Gal, B.K. Jennings, Nucl. Phys. A **594**, 311 (1995).
23. J. Schaffner-Bielich, A. Gal, Phys. Rev. C **62**, 034311 (2000).
24. S. Banik, D. Bandyopadhyay, J. Phys. G **26**, 1495 (2000).
25. J. Negele, D. Vautherin, Nucl. Phys. A **207**, 298 (1973).
26. G. Baym, C. Pethick, P. Sutherland, Astrophys. J. **170**, 299 (1971).
27. I. Vidaña, A. Polls, A. Ramos, L. Engvik, M. Hjorth-Jensen, Phys. Rev. C **62**, 035801 (2000).
28. M. Baldo, G.F. Burgio, H.-J. Schulze, Phys. Rev. C **61**, 055801 (2000).
29. J. Cottam, F. Paerels, M. Mendez, Nature **420**, 51 (2002); D. Sanwal, G.G. Pavlov, V.E. Zavlin, M.A. Teter, Astrophys. J. **574**, L61 (2002).
30. J.A. Pons, S. Reddy, M. Prakash, J.M. Lattimer, J.A. Miralles, Astrophys. J. **513**, 780 (1999).
31. Z. Gong, L. Zejda, W. Däppen, J.M. Aparicio, Comput. Phys. Commun. **136**, 294 (2001); J.M. Aparicio, Astrophys. J. Suppl. **117**, 627 (1998).
32. M. Prakash, I. Bombaci, M. Prakash, P.J. Ellis, J.M. Lattimer, R. Knorren, Phys. Rep. **280**, 1 (1997).
33. S. Reddy, M. Prakash, J.M. Lattimer, Phys. Rev. D **58**, 013009 (1998).
34. I. Vidaña, A. Polls, A. Ramos, H.-J. Schulze, Phys. Rev. **64**, 044301 (2001).
35. I. Vidaña, A. Rios, L. Mornas, A. Polls, A. Ramos, *Parametrization of Brueckner-Hartree-Fock calculations for polarized baryonic matter*, in preparation.
36. I. Vidaña, A. Ramos, A. Polls, Phys. Rev. C **70**, 024306 (2004).
37. N.K. Glendenning, Astrophys. J. **293**, 470 (1985); J. Schaffner, I.N. Mishustin, Phys. Rev. C **53**, 1416 (1996); F. Hofmann, C.M. Keil, H. Lenske, Phys. Rev. C **64**, 025804 (2001).
38. N.K. Glendenning, *Compact Stars* (Springer Verlag, New York, 1997).
39. M. Bender, J. Dobaczewski, J. Engel, W. Nazarewicz, Phys. Rev. C **65**, 054322 (2002).
40. E.S. Hernández, J. Navarro, A. Polls, Nucl. Phys. A **627**, 460 (1997).